AEDC-TR-67-242

OPERATION OF AEDC-VKF 100-IN. HOTSHOT TUNNEL F WITH AIR AS A TEST GAS AND APPLICATION TO SCRAMJET TESTING

I. T. Osgerby and H. K. Smithson

ARO, Inc.

December 1967

VON KÁRMÁN GAS DYNAMICS FACILITY
ARNOLD ENGINEERING DEVELOPMENT CENTER
AIR FORCE SYSTEMS COMMAND
ARNOLD AIR FORCE STATION, TENNESSEE

NOTICES

When U. S. Government drawings specifications, or other data are used for any purpose other than a definitely related Government procurement operation, the Government thereby incurs no responsibility nor any obligation whatsoever, and the fact that the Government may have formulated, furnished, or in any way supplied the said drawings, specifications, or other data, is not to be regarded by implication or otherwise, or in any manner licensing the holder or any other person or corporation, or conveying any rights or permission to manufacture, use, or sell any patented invention that may in any way be related thereto.

Qualified users may obtain copies of this report from the Defense Documentation Center.

References to named commercial products in this report are not to be considered in any sense as an endorsement of the product by the United States Air Force or the Government.

OPERATION OF AEDC-VKF 100-IN. HOTSHOT TUNNEL F WITH AIR AS A TEST GAS AND APPLICATION TO SCRAMJET TESTING

I. T. Osgerby and H. K. Smithson
ARO, Inc.

AF - AEDC
Arnold AFS Tenn

FOREWORD

The research reported herein was sponsored by the Arnold Engineering Development Center (AEDC), Air Force Systems Command (AFSC), under Program Element 6240521F, Project 3012, Task 301207.

The results of research reported herein were obtained by ARO, Inc. (a subsidiary of Sverdrup & Parcel and Associates, Inc.), contract operator of AEDC, AFSC, under Contract AF40(600)-1200. The experimental tests were conducted under ARO Project VT5822, from January 1966 through May 1967, and the manuscript was submitted for publication on October 17, 1967.

The results of this research were presented at the Fifth Hypervelocity Techniques Symposium held at the University of Denver, March 1967.

This technical report has been reviewed and is approved.

Forrest B. Smith
Research Division
Directorate of Plans
and Technology

Edward R. Feicht
Colonel, USAF
Director of Plans
and Technology

ABSTRACT

An experimental and theoretical research program has been undertaken to develop the arc-heated hypervelocity Tunnel F of the von Kármán Gas Dynamics Facility (AEDC) for operation as a combustion test facility with air as a test gas. Preliminary results of this test program are reported concerning gaseous and particle contamination and the limitations on combustion testing attributable to reservoir decay.

CONTENTS

TABLE

ILLUSTRATIONS

NOMENCLATURE

d^*	Throat diameter
k_p	Defined by Eq. (4)
k_T	Defined by Eq. (5)
L_c	Combustion length
L_R	Reaction length
M_∞	Free-stream Mach number
p	Pressure
$\dot{q}_o$	Stagnation point heat-transfer rate
$\dot{q}_o(I)$	Value of $\dot{q}_o$ inferred from $\dot{q}_s$
$\dot{q}_s$	Shoulder heat-transfer rate
R	Radius of hemisphere
S	Distance along surface of hemisphere-cylinder
T	Temperature
t	Time
U	Flow velocity
X	Distance along combustor
ρ	Density
τ_{ID}	Ignition delay time
τ_o	Total combustion time
τ_R	Reaction time

SUBSCRIPTS

1, 2, 3	See Fig. 15
o	Reservoir
∞	Free stream

SUPERSCRIPT

$'$	Value behind a normal shock

SECTION I
INTRODUCTION

Tunnel F of the von Kármán Gas Dynamics Facility (VKF) (Refs. 1 and 2) is an arc-heated hypervelocity (hotshot) tunnel with a 100-in.-diam main test section. In terms of Mach number and Reynolds number, a wide range of flight conditions is simulated, using nitrogen as the test gas (Refs. 3 through 9). A useful run time between 50 and 100 msec is attained.

A program is underway to evaluate the feasibility of using this tunnel for testing integrated SCRAMjets. It is possible to determine the boundary-layer characteristics of a SCRAMjet inlet in cold flow tunnels, which simulate Mach number and Reynolds number, and it is possible to test the combustor in present high enthalpy facilities, e.g. shock tunnels. There are, however, very critical problems arising on the integration of these two components, such as the effect of the boundary layer at the combustor inlet on the combustion process, which requires tests of a complete integrated model. In order to study the integrated unit experimentally, a facility must have adequate Mach number-Reynolds number capability, at sufficiently high stagnation temperature to permit spontaneous combustion in the combustor. Air must be used as the test gas, and sufficient run time must be available to ensure quasi-steady testing. Shock tunnels offer a capability for testing SCRAMjet components and systems, but the available run time and other operational problems limit their usefulness for such application. Hotshot tunnels appear attractive for tests at higher velocities, because of the long run time, relatively high stagnation temperatures (up to 4000°K), and high stagnation pressure (up to 40,000 psia).

The capability of the AEDC-VKF hotshots as aerodynamic test devices for the usual aerodynamic studies, i.e. static stability, pressure distributions, and heat-transfer distributions, has been clearly established (Refs. 1 through 9); however, this work was all accomplished using nitrogen as the test gas. During the early history of the AEDC hotshot tunnels, nitrogen was substituted for air as a test gas because of excessive oxygen depletion. During the early attempts to use air as a test gas, the test section oxygen content was observed to be as low as 4 to 8 percent for some arc-chamber configurations (Ref. 9). Development work over the past several years has led to marked improvements in arc-chamber design, materials of construction and operating techniques, so that with the current interest in SCRAMjet- type vehicles it is appropriate to examine the feasibility of using air as a test gas in the current hotshot tunnels.

In addition to the problem of oxygen depletion inherent in hotshots with air as the test gas, there are other potential problems associated with these tunnels. There is a decay of state parameters in the reservoir (e.g. temperature, pressure) which can be more serious for combustion testing than for aerodynamic testing. In addition, the effects of contaminants on the combustion process need study. This report presents the current results of studies from a continuing research program on these three topics, with hydrogen as the fuel.

SECTION II
TEST APPARATUS

2.1 TUNNEL

Tunnel F (Figs. 1 and 2) is a hotshot-type tunnel with a 100-in.-diam main test section. The test gas is initially confined in an arc-chamber by a diaphragm located near the throat of an attached conical nozzle. This nozzle has a total included angle of 8 deg. The gas is heated by an electric arc discharge and expanded through the conical nozzle to the test section. The energy for the electric arc is furnished by an inductive power supply with a maximum energy storage capability of 100 million joules.

Most of the experimental data given in this report were obtained in the 100-in. test section. Some gas samples were taken at an upstream 54-in. test section (see Fig. 2). Computed combustion test capabilities are given for both test section locations later in the report.

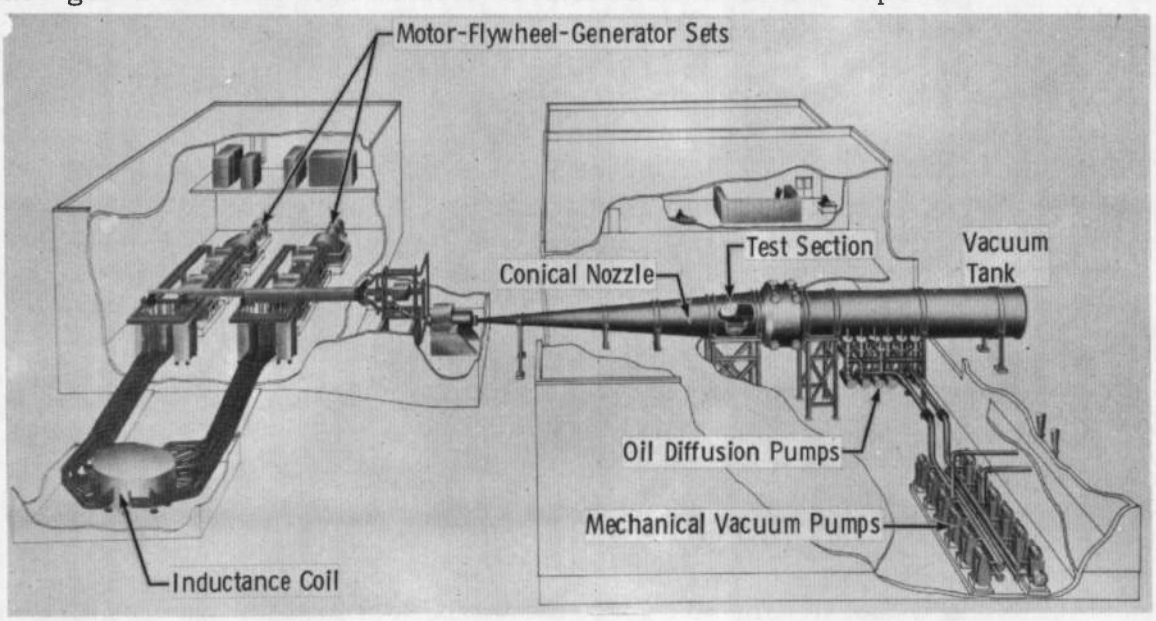

Fig. 1 Tunnel F

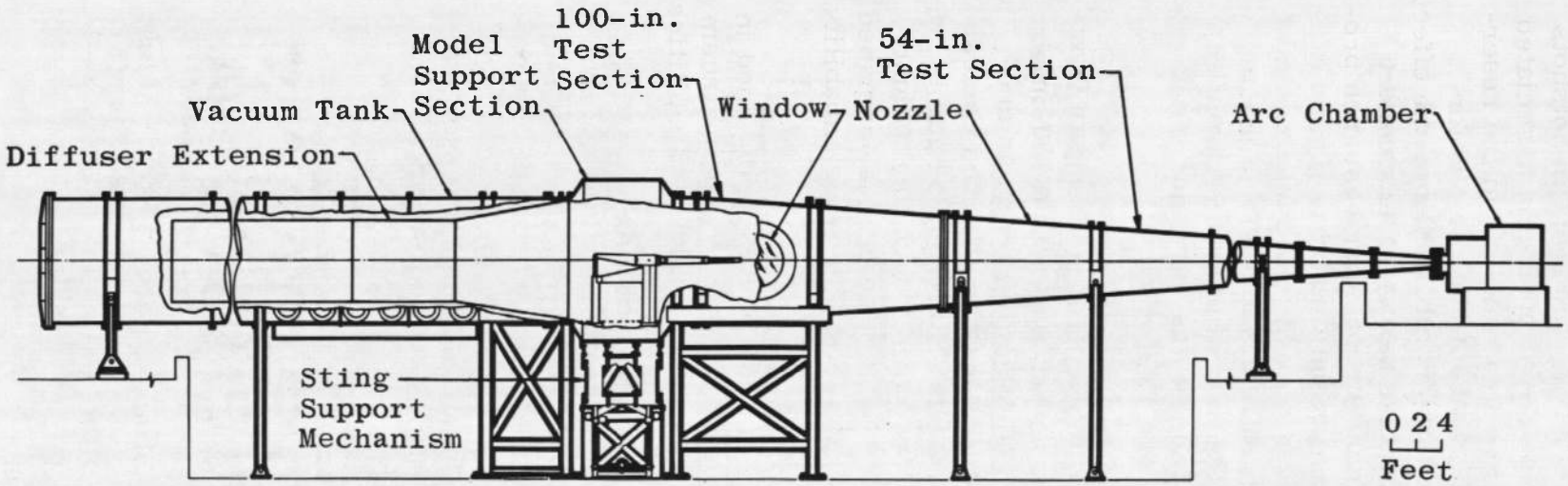

Assembly

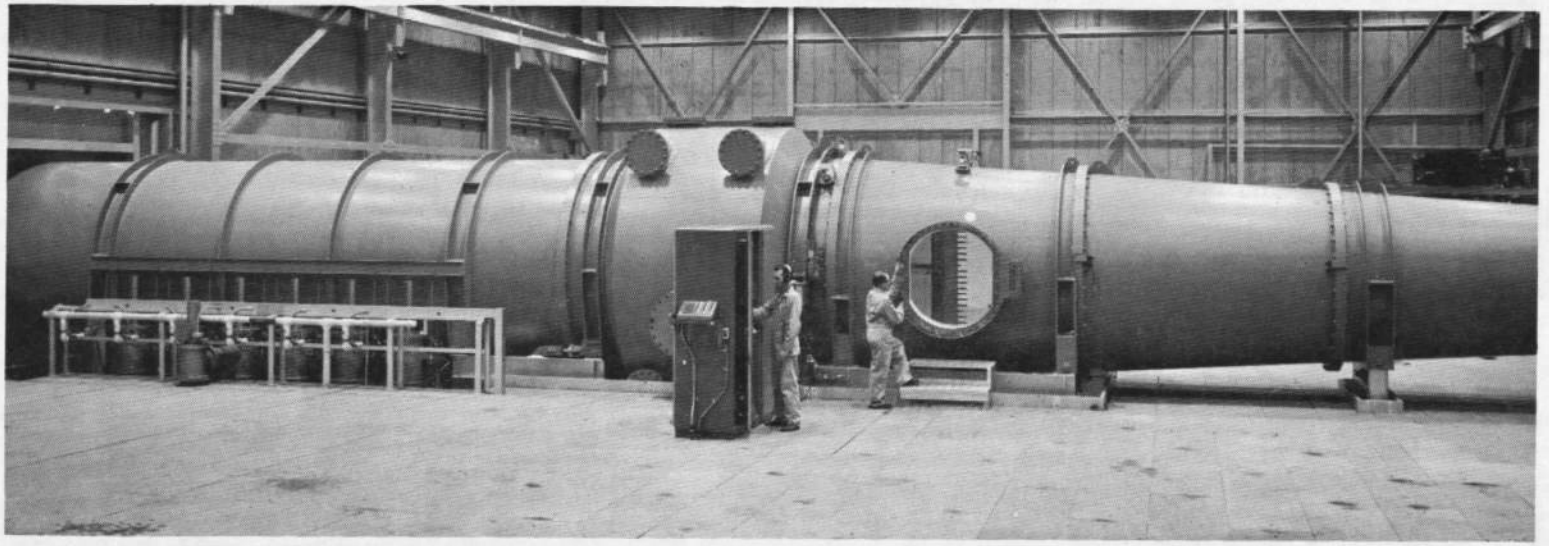

Fig. 2 100-in. Hypervelocity Tunnel F

2.2 ARC-CHAMBER AND BAFFLES

The arc-chamber is shown in the upper half of Fig. 3. When the inductive energy supply is switched to the arc-chamber, the magnetic fuse opens and initiates an arc. The electrical energy is released in about 12 to 30 msec. The arcing is a random process and cannot be expected to heat the gas uniformly. Thus, the uniformity of the reservoir gases depends strongly on the degree of mixing which takes place before the gases expand through the nozzle throat. A baffle is placed in front of the throat entrance to prevent the arc striking the throat and is designed to promote further mixing of the gas to reduce local enthalpy gradients caused by asymmetric arc-heating.

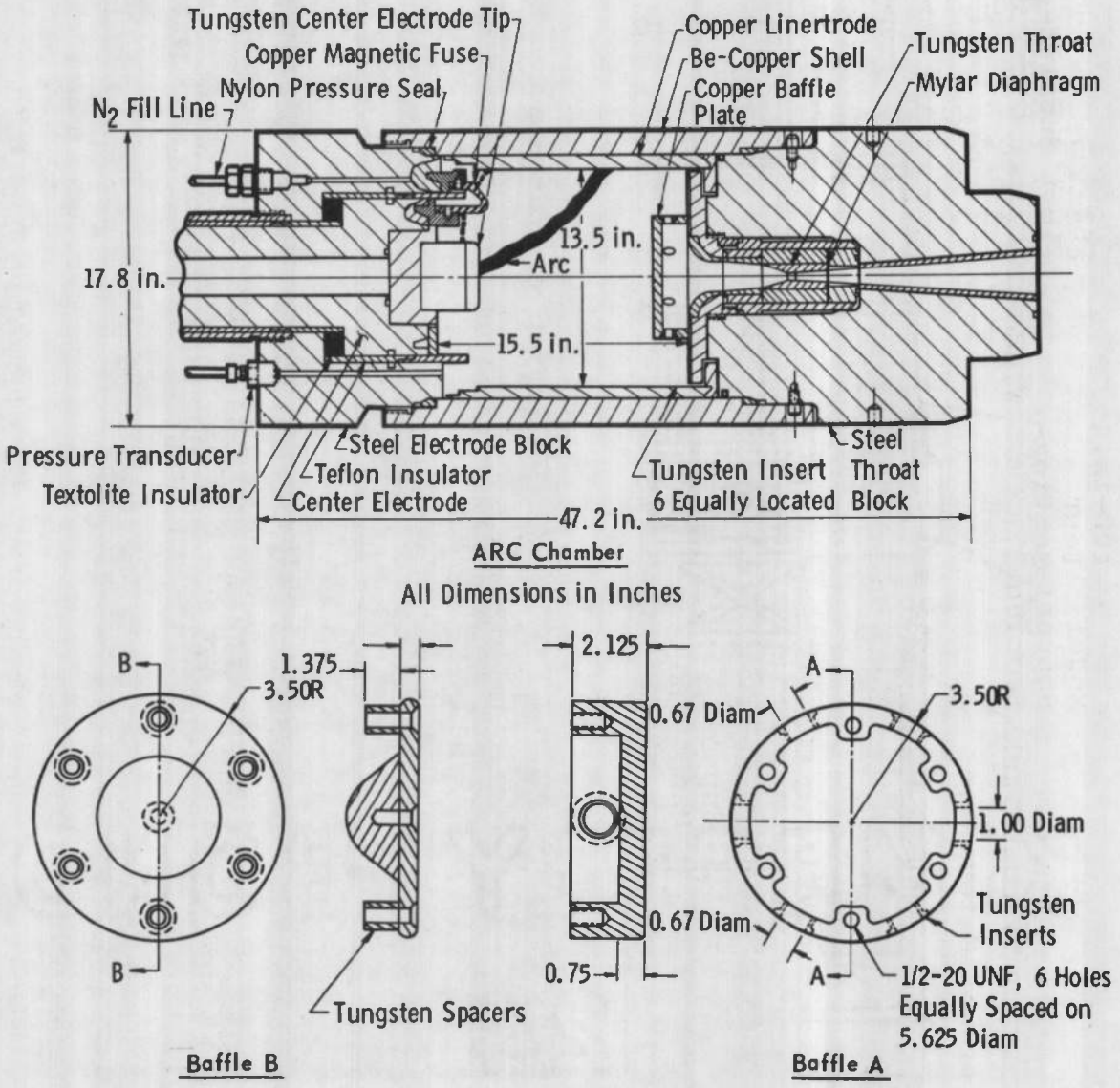

Fig. 3 Arc Chamber

Several baffle designs were used during the tests reported here, two of which are shown in Fig. 3. Baffle A had six entrance ports, four of which were 0.67-in. diameter and two of which were 1.0-in. diameter. Baffle B had open sides. Baffle C, which was a modified form of baffle A (the 1.0-in.-diam ports were replaced with 0.67-in.-diam ports), was used but found to be too restrictive since the contamination increased relative to baffles A and B. For maximum effectiveness, an individual baffle design would be required for a particular reservoir condition. Baffle A gave good results for the tests presented here.

2.3 PROBES AND RAKE

Heat-transfer measurements were made using slug calorimeters. The calorimeter consists of a platinum thin film resistance thermometer deposited on an anodized aluminum disk as shown in Fig. 4. These heat-transfer transducers have been used with a high degree of confidence in impulse-type wind tunnels. Reference 2 gives additional details on the use of these transducers. Measurements were made at the stagnation point and the shoulder of a hemisphere-cylinder as shown in Fig. 5.

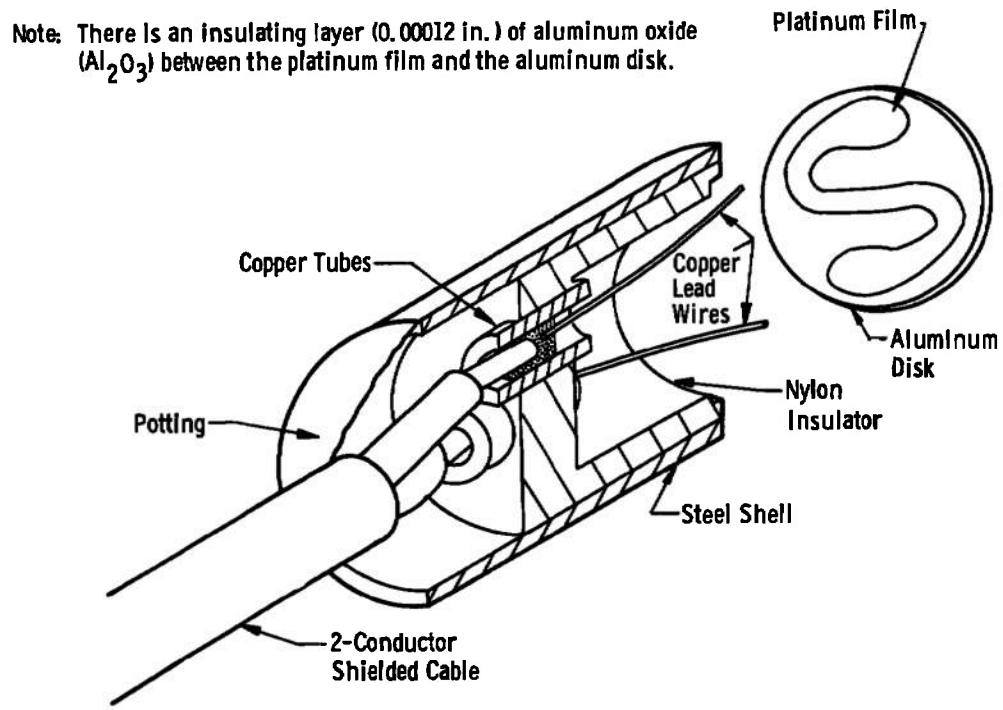

Fig. 4 Slug Calorimeter with Thin Film Resistance Thermometer Temperature Sensor

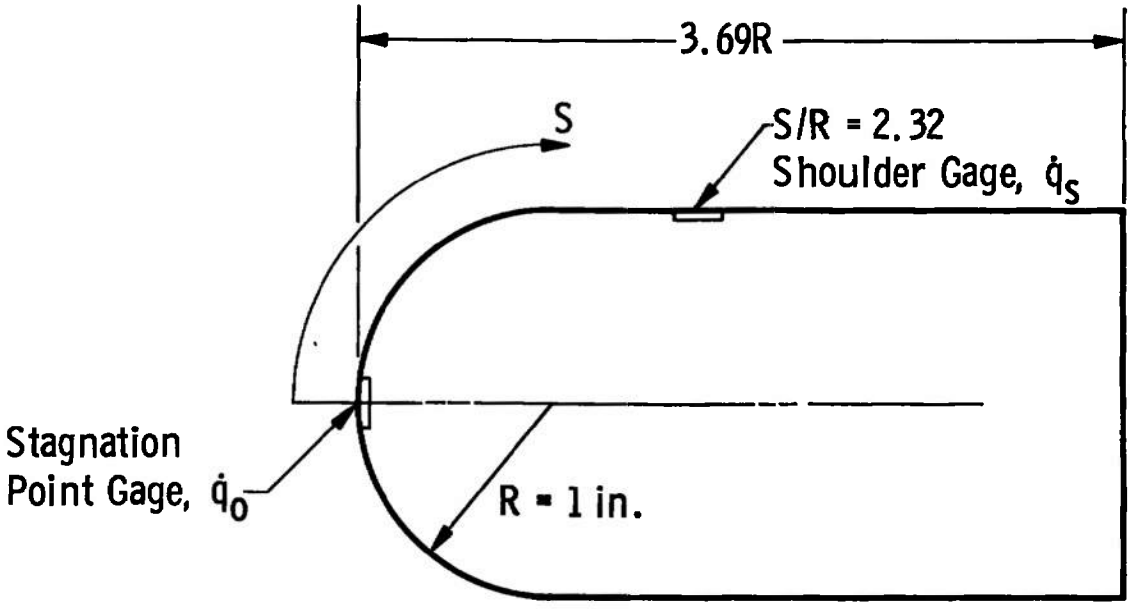

Fig. 5 Hemisphere-Cylinder Heat-Transfer Probe

Pitot pressures were measured using semiconductor strain-gage-type transducers. The transducer is a differential pressure measuring device shown in Fig. 6. The differential pressure is transmitted through a flexible latex diaphragm to a cantilevered beam. Two semiconductor strain gages sense the deflection of the beam. Additional information on the pressure transducers may be found in Ref. 10. A drawing of the rake installation is shown in Fig. 7.

2.4 GAS SAMPLING ASSEMBLY

The location of the gas sampling assembly is shown in Fig. 7, and a diagram of the assembly is shown in Fig. 8. The assembly contained two glass sample bottles with vacuum stopcocks. Flow of gas into these bottles was controlled by solenoid actuated valves. "Start" and "run" gas samples were obtained. The start sample was taken during the initial starting process and required a two-way valve (normally closed). A three-way valve was required for the run sample in order to establish flow through the pitot tube and spill the gas flow until a sample was desired.

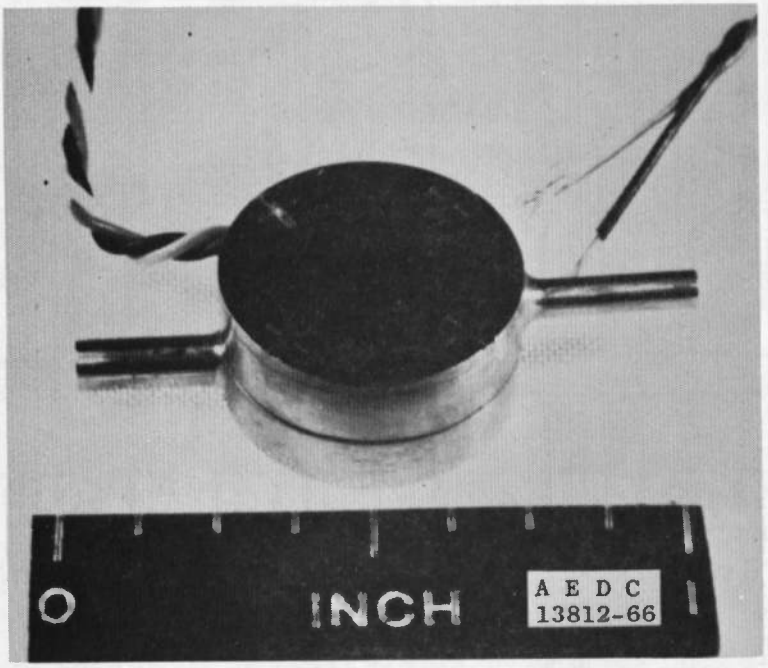

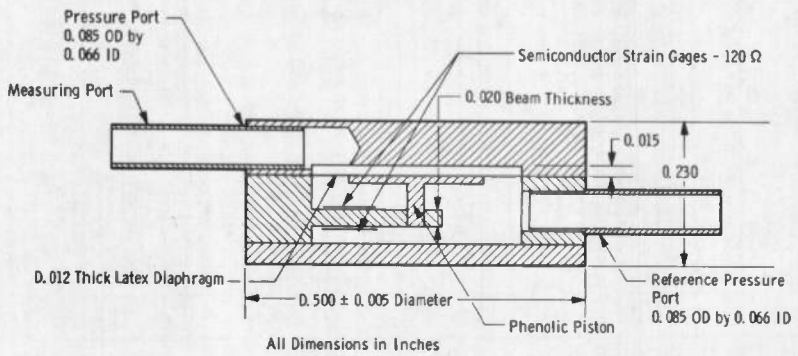

Fig. 6 Pressure Transducer

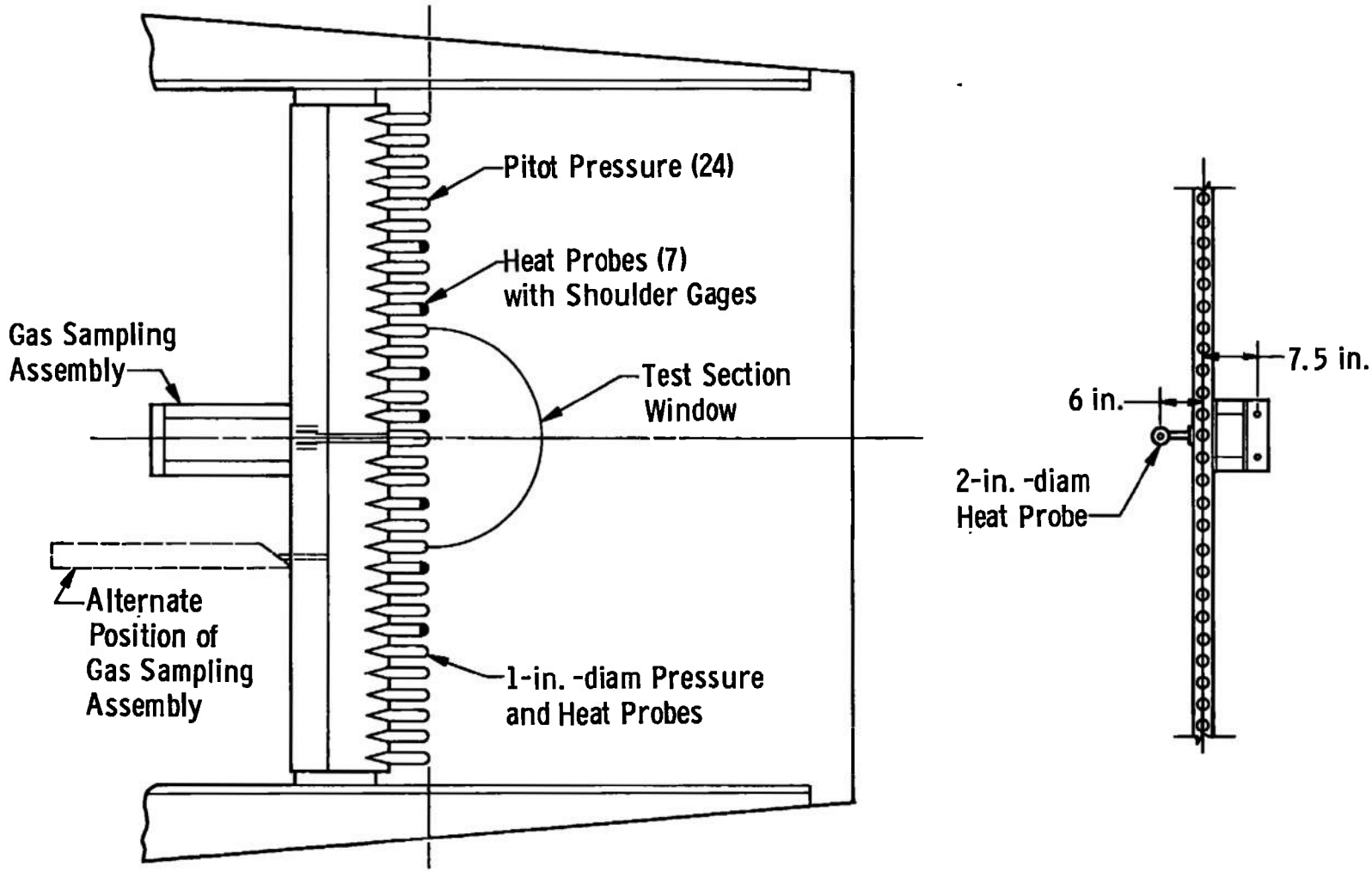

Fig. 7 Installation and Instrumentation of Tunnel F Rake

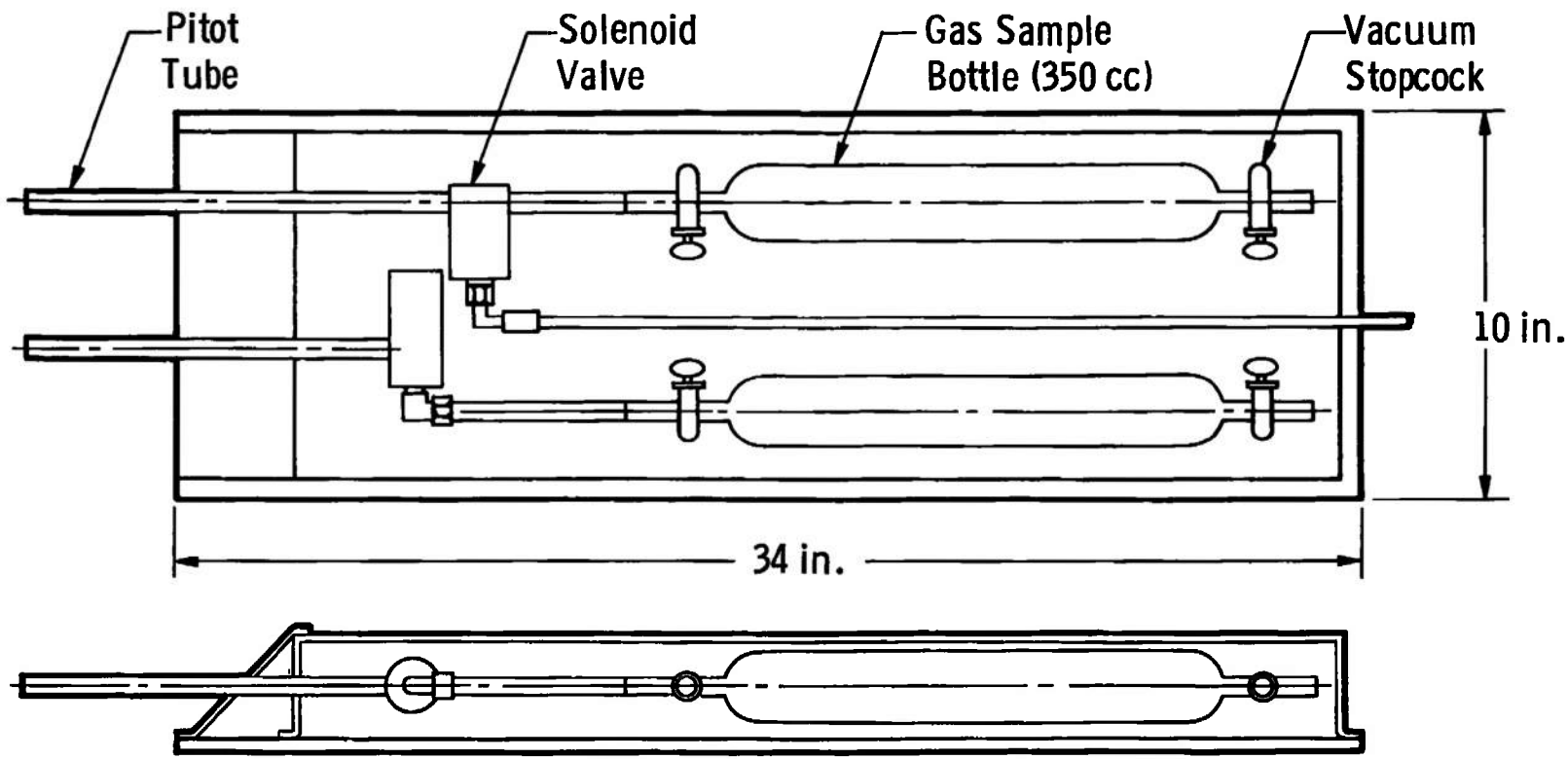

Fig. 8 Tunnel F Gas Sampling Assembly

The gas sampling bottles were outgassed at a temperature of 100°C or higher and at a vacuum of about 0.1 torr for a period of one hour. After the sampling bottles were installed, they were opened at an evacuated tunnel pressure of 0.01 torr or less in order to evacuate residual gases in the sampling system. The valve positions and sampling times for a typical run are shown in Fig. 9. Sampling times varied from about 15 to 38 msec. The collected sample pressures varied from about 1 to 6 torr. The gas samples were analyzed by an Associated Electrical Industries mass spectrometer. The accuracy of mass spectrographic analysis was estimated to be within 1 percent for a sample pressure of 0.1 torr or higher. The overall accuracy of the gas samples was estimated to be within 5 percent.

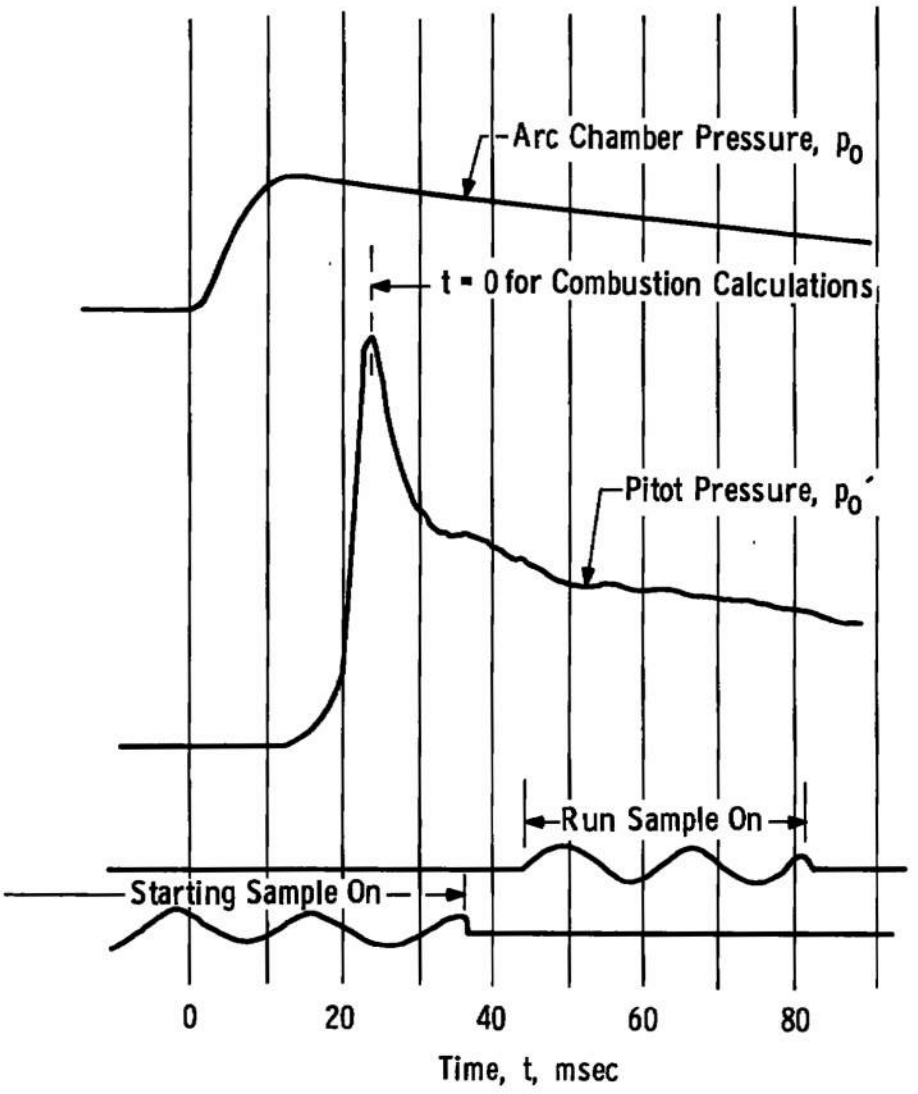

Fig. 9 Typical Run Trace-Gas Sample Timing

SECTION III
TEST RESULTS

3.1 GAS COMPOSITION

Results of the test section gas sample analyses are shown in Table I.

TABLE I
GAS SAMPLE ANALYSIS

Run Conditions					Composition by Volume								
p_o, psia	T_o', °K	ρ_o', amagat	d*, in.	Baffle†	N_2	O_2	A	CO_2	H_2	H_2O	NO	Type Sample**	
8,119	2950	0.004	0.48	B	79.0	16.9	1.00	0.3	---	---	2.9	S	100-in.
					77.1	17.9	0.90	0.4	---	0.2	3.6	R	Test
8,410	3200	0.004	0.48	C	78.6	18.9	0.90	0.2	---	0.2	1.2	S	Section
					77.4	17.7	0.90	0.3	---	0.2	3.5	R	
8,168	2850	0.004	0.48	B	80.3	15.6	0.90	0.7	---	0.1	2.2	S	
					78.6	17.1	0.84	0.5	---	---	2.7	R	
9,380	3050	0.004	0.48	B	77.9	18.4	0.9	0.4	0.3	---	2.3	S	
					81.2	16.2	0.9	0.6	0.7	---	1.5	R	
8,002	2800	0.006	0.69	B	81.1	16.0	0.9	0.5	---	---	1.3	S	
					78.2	18.9	0.9	0.5	---	---	1.5	R	
7,870	3050	0.006	0.69	C	80.8	16.7	0.9	0.5	---	---	1.0	S	
					82.3	13.7	0.9	0.6	---	---	1.9	R	
6,460	2610	0.006	0.91	B	77.8	19.3	0.9	0.6	---	---	1.4	S	
					80.4	19.7	0.9	1.1	---	---	2.9	R	
7,348	2064	0.01	0.91	B	81.3	16.7	1.0	0.3	---	0.4	0.4	S	
					78.7	19.1	0.9	0.9	---	0.1	0.5	R	
9,353	2008	0.01	0.69	A	78.5	19.6	0.9	0.5	0.5	---	---	S	
					78.5	20.1	0.9	0.6	0.6	0.5	0.2	R	
9,273	2387	0.01	0.69	A	78.3	19.3	0.9	0.5	0.5	---	0.4	S	
					77.6	20.1	0.9	0.8	0.5	---	0.6	R	
9,528	2377	0.01	0.69	A	77.4	20.5	0.9	0.8	---	---	0.3	S	
					78.2	20.9	0.9	0.5	---	---	0.4	R	
9,560	2154	0.01	0.69	A	77.8	19.1	0.9	0.2	0.4	---	0.6	S	
					78.3	20.1	0.9	0.4	0.2	---	0.4	R	
9,864	1878	0.01	0.69	A	77.4	18.7	0.9	0.4	0.2	---	0.4	S	
					78.9	19.8	0.9	0.9	0.2	---	0.4	R	
9,776	2020	0.01	0.69	A	78.1	19.3	0.9	0.4	0.2	---	1.0	S	
					76.4	20.7	0.9	0.9	0.4	---	0.7	R	
7,200	2269	0.01	0.69	A	77.2	21.3	0.9	---	---	---	1.7	R	54-in.
8,203	1957	0.05	0.69	A	78.7	20.7	0.9	---	---	---	1.1	R	Test Section
10,966	2155	0.04	0.69	A	74.6	19.8	0.9	---	---	---	0.6	R	
10,500	2559	0.03	0.69	A	78.1	19.3	0.9	---	---	---	1.4	R	
- DRY AIR					78.2	20.9	0.9	---	---	---	---	-	

**S - Start Sample
R - Run Sample
†See Fig. 3

Because of density and enthalpy decay of the reservoir, each sample was collected during a period of varying total conditions. The parameters T_o' and ρ_o' represent average values of the temperature and density behind the normal shock on the pitot sampling tube during the sampling

period. The temperature and density at the stagnation point are determined by iteration, using measured values of reservoir pressure, p_o, pitot pressure, p'_o, and stagnation point heat-transfer rate*, $\dot{q}_o$. The data reduction procedure is described in Ref. 7. For total temperatures in excess of 3000°K, the oxygen content was 17 to 18 percent compared to 20.9 percent for dry air. There were no systematic differences noted between "start" and "run" samples.

In Fig. 10, the percent oxygen by volume is plotted versus the stagnation point temperature, T'_o, which is approximately equal to the reservoir temperature, T_o. The scatter is fairly high, but there is some reduction in the oxygen content at increasing temperatures.

These initial results are encouraging, in that the large amounts of oxygen depletion encountered in the past when testing in hotshot tunnels with air have been reduced to more reasonable values. With further effort in baffle design, additional improvements are expected.

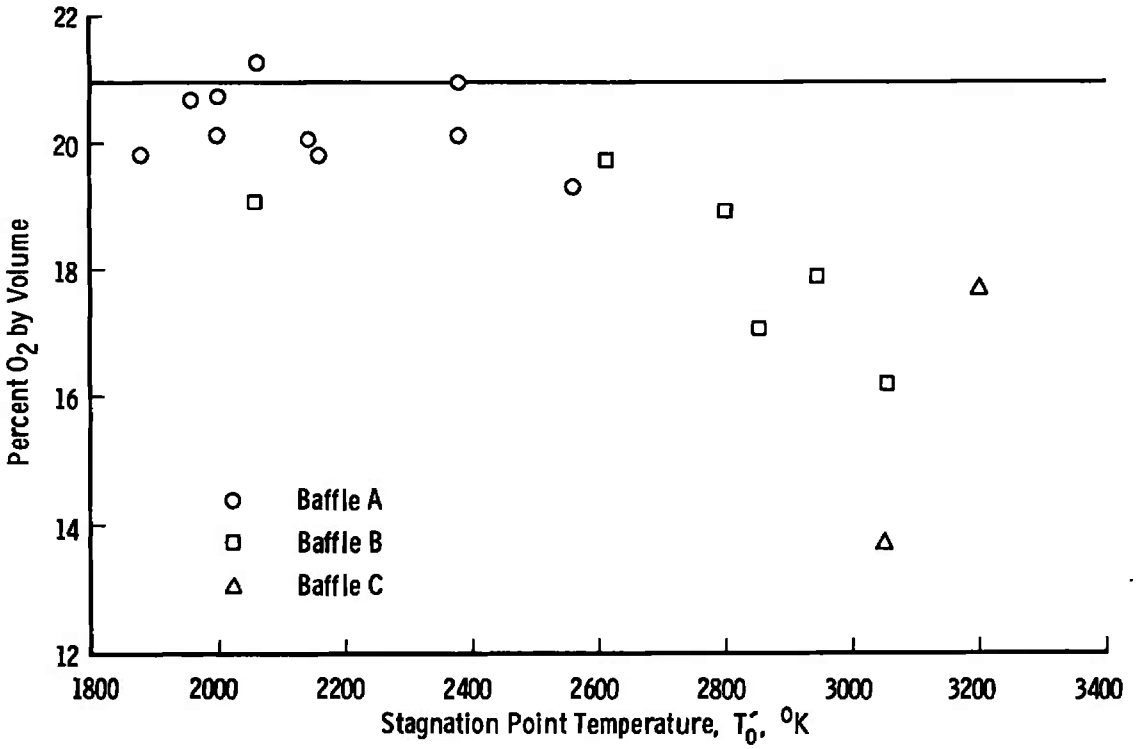

Fig. 10 Oxygen Content of Test Gas

*The catalytic effects on the measured heat-transfer rate were estimated to be small and thus were neglected.

3.2 PARTICLE CONTAMINATION

A dual heat-transfer-probe (hemisphere-cylinder, Fig. 5) was used to monitor particle contamination (Refs. 7 and 8). When the flowing gas contains solid particles, the stagnation-point heat-transfer rate will be higher than the corresponding heat-transfer rate for uncontaminated flow, because of particles impinging on the heat-transfer gage. The corresponding influence of particles on a shoulder heat-transfer gage may be assumed to be relatively small. Thus, a comparison of the measured stagnation point heat-transfer rate, $\dot{q}_o$, with the theoretical value inferred from the measured heat-transfer rate to the shoulder gage, $\dot{q}_o(I)$, may be used as a monitor of particle contamination (i.e., $\dot{q}_o(I) = \dot{q}_s/0.050$). Typically, with "clean" nitrogen runs, these values agree within ±10 percent (Ref. 7). For one series of air tests at high total temperatures, the ratio of measured to inferred stagnation point heat-transfer rate indicated a significant increase in particle contamination. The particle contamination monitor $\dot{q}_o/\dot{q}_o(I)$ is plotted against total temperature in Fig. 11 and against oxygen concentration in Fig. 12. The use of baffle design A (Fig. 3) reduced the contamination level appreciably. With baffle B, values of $\dot{q}_o/\dot{q}_o(I)$ average about 1.3 compared with an average of about 1.08 with baffle A. Test section oxygen concentration with baffle B was about 18 percent and with baffle A about 20 percent. It was evident that considerable oxidation occurred in the arc-chamber and nozzle throat (as confirmed by visual inspection after each test). Baffle A design indicated a marked reduction in contamination level. The improvement in baffle design forces the gas through six equally spaced holes; thus, better mixing of the gas should result. The tungsten inserts, with rounded entrance ports, definitely reduced spalling and erosion of the baffle as confirmed by inspection after a test, thus significantly reducing the amount of oxidation occurring in the arc-chamber.

3.3 FLOW UNIFORMITY

Pitot pressure profiles were measured in the 100-in. test section to determine flow uniformity. Profiles of the pitot pressure surveys, referenced to the reservoir pressure, are presented for the three nozzle throat sizes in Fig. 13. The uniformity was satisfactory for all throat sizes tested. The pitot pressure variation over a 50-in. test core was about ±5 percent. The pressure profiles were similar to those obtained for nitrogen runs (Refs. 1 and 2).

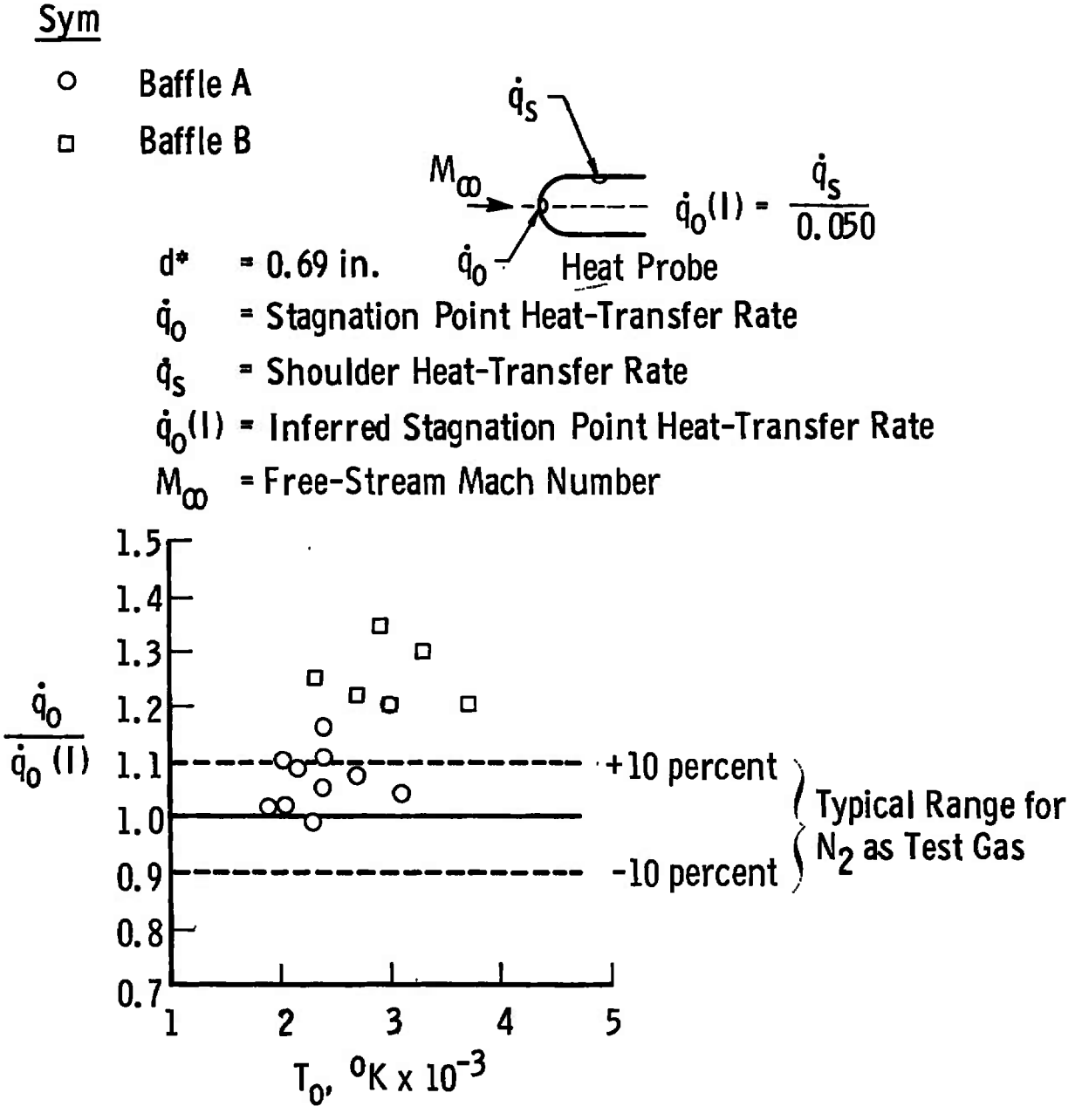

Fig. 11 Effect of Reservoir Temperature on Particle Contamination with Air as Test Gas

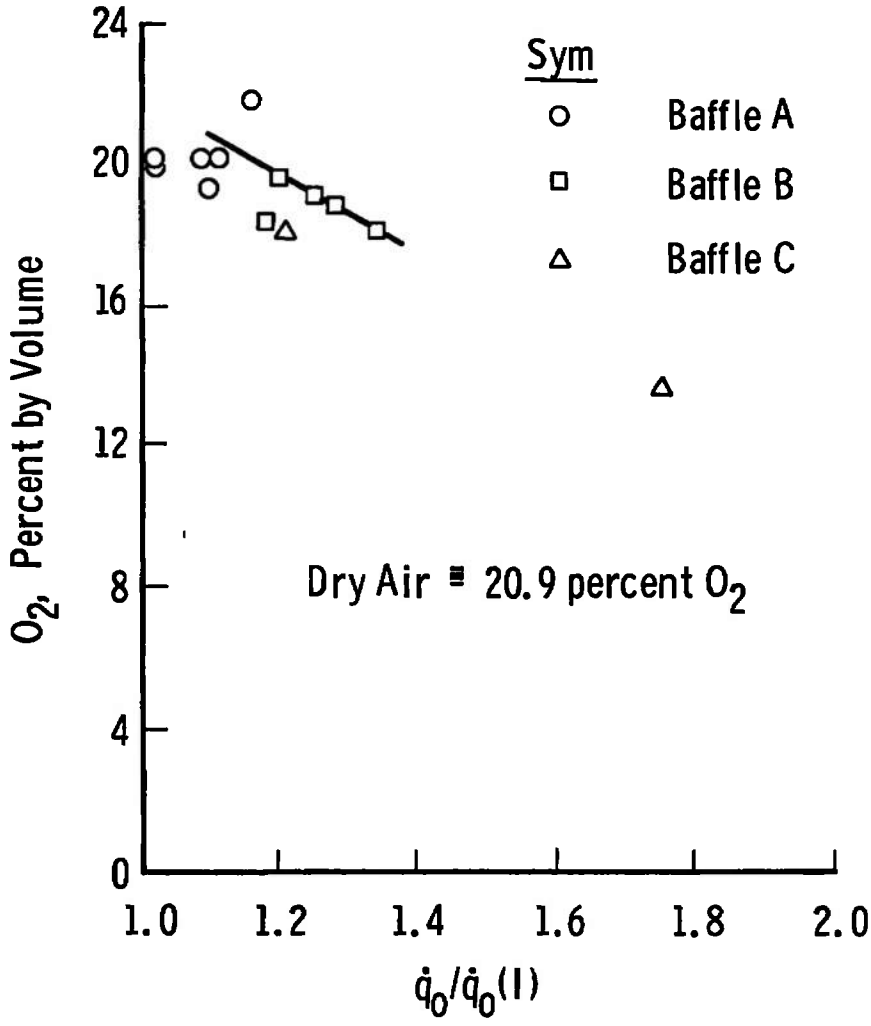

Fig. 12 Effect of Contamination on Oxygen Content of the Test Section Gas Sample

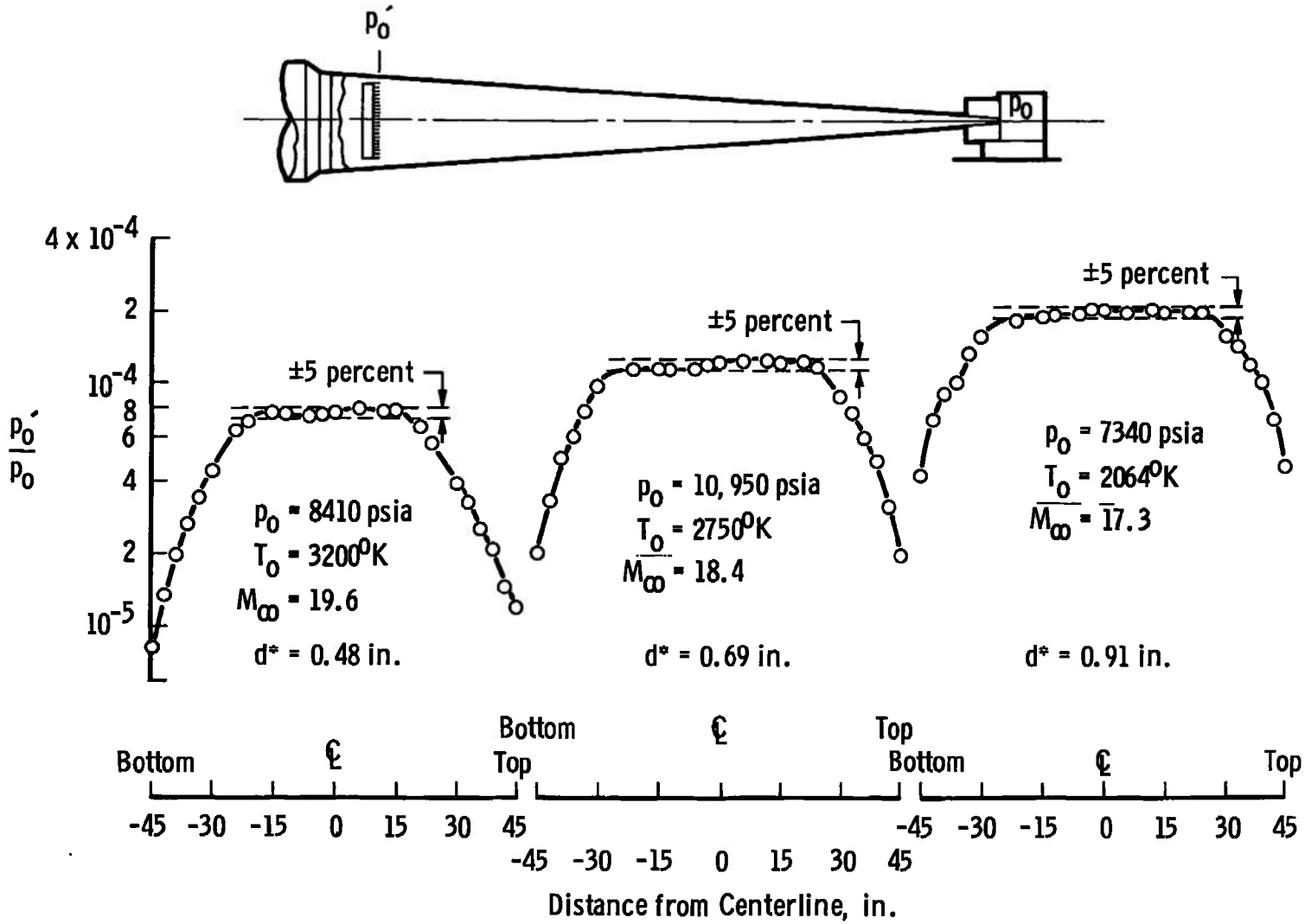

Fig. 13 Pressure Profile in Vertical Plane at Test Section

SECTION IV
THEORETICAL CONSIDERATIONS

4.1 EFFECT OF RESERVOIR DECAY ON COMBUSTION TESTING

Since a hotshot tunnel involves expansion of a gas from a constant volume reservoir, the reservoir temperature and pressure decrease with time. This decay is much more serious for combustion testing than for aerodynamic testing, because of the strong dependence of the reaction rates on both temperature and pressure.

One parameter used here to estimate the duration of useful run time is the rate of change of combustor length relative to the flow velocity. Testing in the quasi-steady mode requires that this parameter be less than some value. Based upon previous aerodynamic work, an upper limit of 0.1 is provisionally chosen for this parameter. If the flow velocity is U, and the combustion length L_c, then this requirement is

$$\frac{1}{U}\frac{d\,L_c}{dt} < 0.1$$

The combustion length can be related to the ignition delays and reaction times by

$$L_c = U\,\tau_o$$

where τ_o is the time required for 95-percent complete combustion. The time for combustion can be estimated as the sum of two parts: (1) an ignition delay, τ_{ID}, and (2) a reaction period, τ_R. These may be related to the static pressure and static temperature in the combustion chamber. Expressions for the ignition delay and reaction time for constant pressure combustion of hydrogen in air have been given in Ref. 11. These expressions are:

$$p\,\tau_{ID} = 8. \times 10^{-3}\, e^{9600/T} \tag{1}$$

and

$$p^{1.7}\,\tau_R = 105\, e^{-1.12T/1000} \tag{2}$$

in which

p is the static pressure, atm

T is the static temperature, °K

τ_{ID} and τ_R, μsec

The time required for combustion is the sum of these

$$\tau_o = \tau_{ID} + \tau_R \tag{3}$$

Values given by Eqs. (1) and (2) are shown in Fig. 14. It is seen from this figure that changes in temperature of a few hundred degrees lead to small changes in the reaction time and large changes in the ignition delay time.

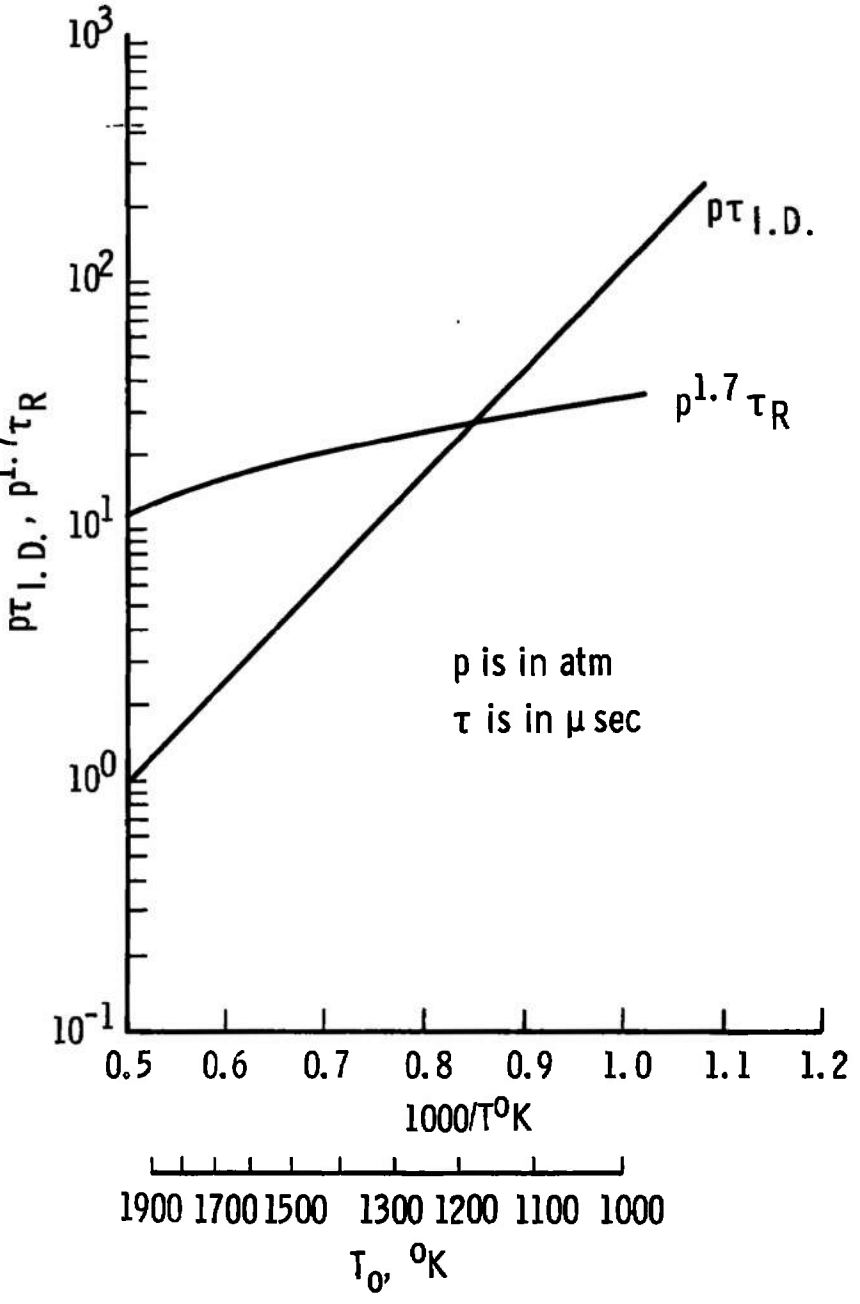

Fig. 14 Ignition (τ_{ID}) and Combustion Time (τ_R)

The values of pressure and temperature to be used in the above equations are the static values at the entrance to the combustor, denoted by (3) in Fig. 15. Figure 15 is a schematic of the simplified model of an integrated SCRAMjet, discussed in this report, having a wedge inlet angle δ_1, and a cowl lip angle δ_2. The static pressure and temperature in the combustor can be related to the free-stream Mach number and the angles δ_1 and δ_2 through which the flow is turned in a simple two shock inlet.

Symbolically

$$\frac{p_3}{P_o} = f(M_\infty, \delta_1, \delta_2) = k_p \tag{4}$$

$$\frac{T_3}{T_o} = f(M_\infty, \delta_1, \delta_2) = k_T \tag{5}$$

These relations may be determined easily for the case of an ideal gas, and results obtained by using Ref. 12 for the case $\delta_1 = \delta_2$ are presented in Figs. 16 and 17.

The effects of a decay in total pressure and temperature on combustion during a test can be estimated with the use of Eqs. (1) through (5). If we assume that the fuel and air mix perfectly just downstream of the fuel injector in the combustor (in practice this would not occur; however, the assumption simplifies the analytical model considerably), then a prescribed length, $L_{ID} = u_3 \times \tau_{ID}$, is taken by the ignition delay and a further length, $L_R = u_3 \times \tau_R$, is required for the reaction period. These are shown schematically in Fig. 18. The values of τ_{ID} and τ_R are obtained from Eqs. (1) and (2) using values of p and T calculated from Eqs. (4) and (5). As the reservoir conditions decay during a test, the values of P_o and T_o decrease; and hence, p_3 and T_3 decrease, causing τ_{ID} and τ_R to increase and hence L_{ID} and L_R to increase.

4.2 RESULTS FOR TUNNEL F

Equations (1) through (5) were used to determine combustor lengths for conditions in Tunnel F, taking into account the decay in reservoir conditions. This was accomplished by using empirical fits to existing experimental data of reservoir decay rates taken from many tests in the VKF hotshot tunnels. The empirical fits relate the total pressure or temperature at time t, to the initial maximum values (where t is set equal to zero).

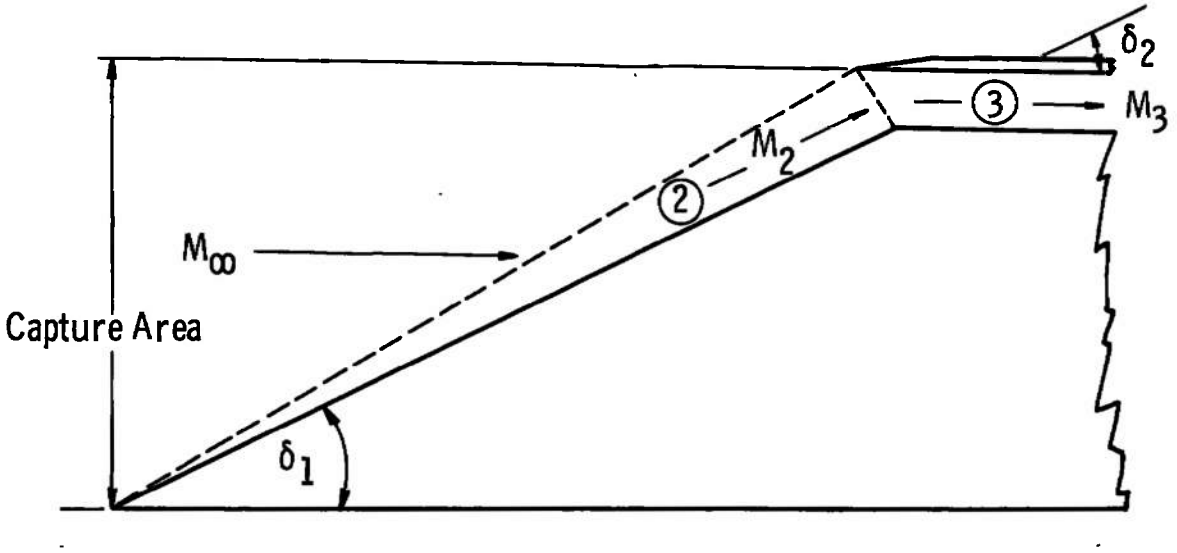

Fig. 15 Schematic of a Two-Shock-Wedge Intake Diffuser

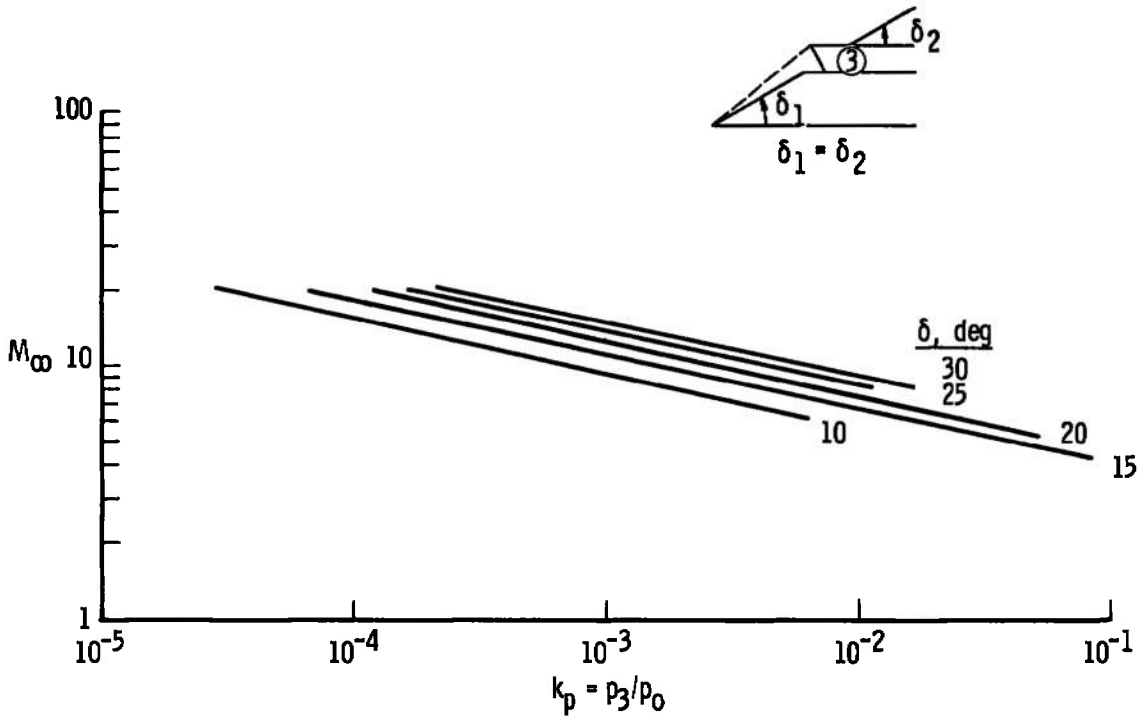

Fig. 16 Static Pressure behind a Two-Shock-Wedge Intake Diffuser ($\gamma = 1.4$)

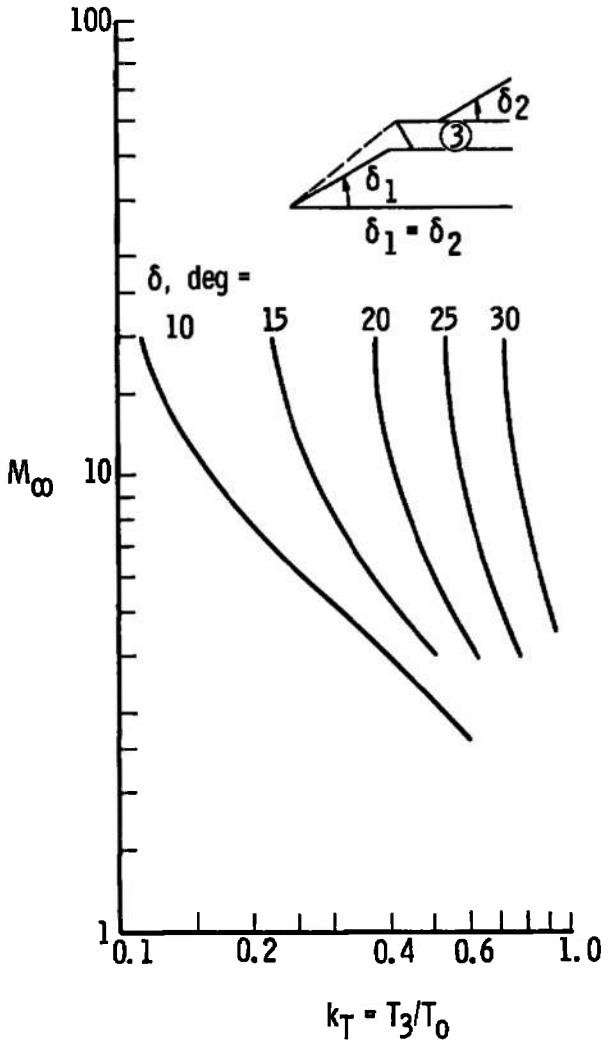

Fig. 17 Static Temperature behind a Two-Shock Wedge Intake Diffuser (γ = 1.4)

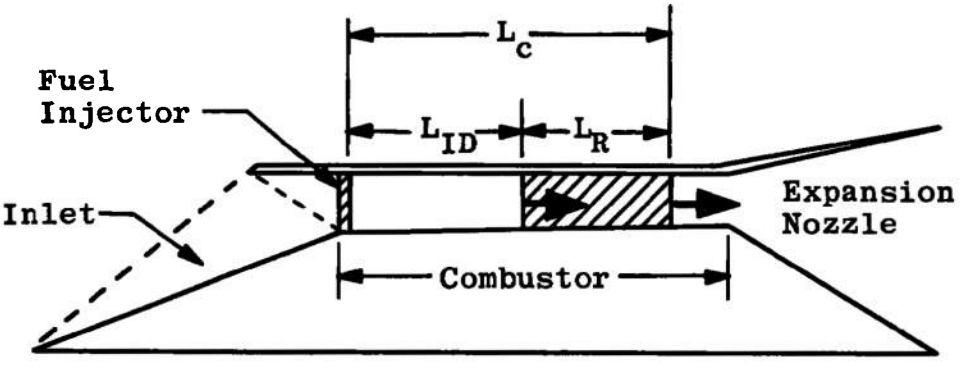

Fig. 18 Details of Quasi-Steady Combustion Process

The reservoir conditions chosen were a total temperature of 4000°K maximum and a total pressure of 40,000 psia maximum. These are limiting conditions which have not as yet been attained simultaneously but have been attained independently with nitrogen as the test gas. The empirical fits were extrapolated to the conditions mentioned above and have been plotted in Fig. 19. The corresponding test section conditions used were:

A. 100-in. test section, $M_\infty = 18$ ($d^* = 0.69$ in.)

B. 54-in. test section, $M_\infty = 12$ ($d^* = 0.95$ in.)

C. 54-in. test section, $M_\infty = 14$ ($d^* = 0.69$ in.)

The latter two conditions correspond to testing at the upstream test section of Fig. 2.

The wedge angles δ_1 and δ_2 were taken to be equal, and a value of 20 deg was assumed. This leads to a constant area combustor, rather than the constant pressure combustor for which Eqs. 1 and 2 apply, but the differences are relatively minor for the present analysis. The combustor lengths for a constant area combustor will be slightly less than those for a constant pressure combustor, because of the increases in temperature and pressure (Ref. 13).

An angle of 20 deg was used throughout since this leads to reasonable estimates of the length required for combustion for a good proportion of the test time available at the 54-in. test section. Higher wedge angles would result in shorter lengths because of the higher ratios of pressure and temperature across the shock waves, but the rate of change of the length during a test would also be increased by the same ratios.

Results of the estimates of combustion lengths are given in Figs. 20, 21, and 22. The total combustion length L_C, obtained from

$$L_C = U_3 \tau_0$$

is shown as a function of time. Also shown is the reaction length, L_R, to be discussed later. The first 20 to 30 msec are taken up in the starting process (Fig. 9) where the zero time corresponds to the reservoir maximum conditions (see Fig. 9). For the highest Mach number case, $M_\infty = 18$ (Fig. 20), the combustion length changes by a factor of two during the time interval from 30 to 50 msec. The lowest Mach number case shown, $M_\infty = 12$ (Fig. 21) has smaller values for the lengths, but the lengths are changing rapidly. The curves are terminated when the combustor entrance static temperature drops below 1000°K. The intermediate Mach number case, $M_\infty = 14$ (Fig. 22), yields smaller changes.

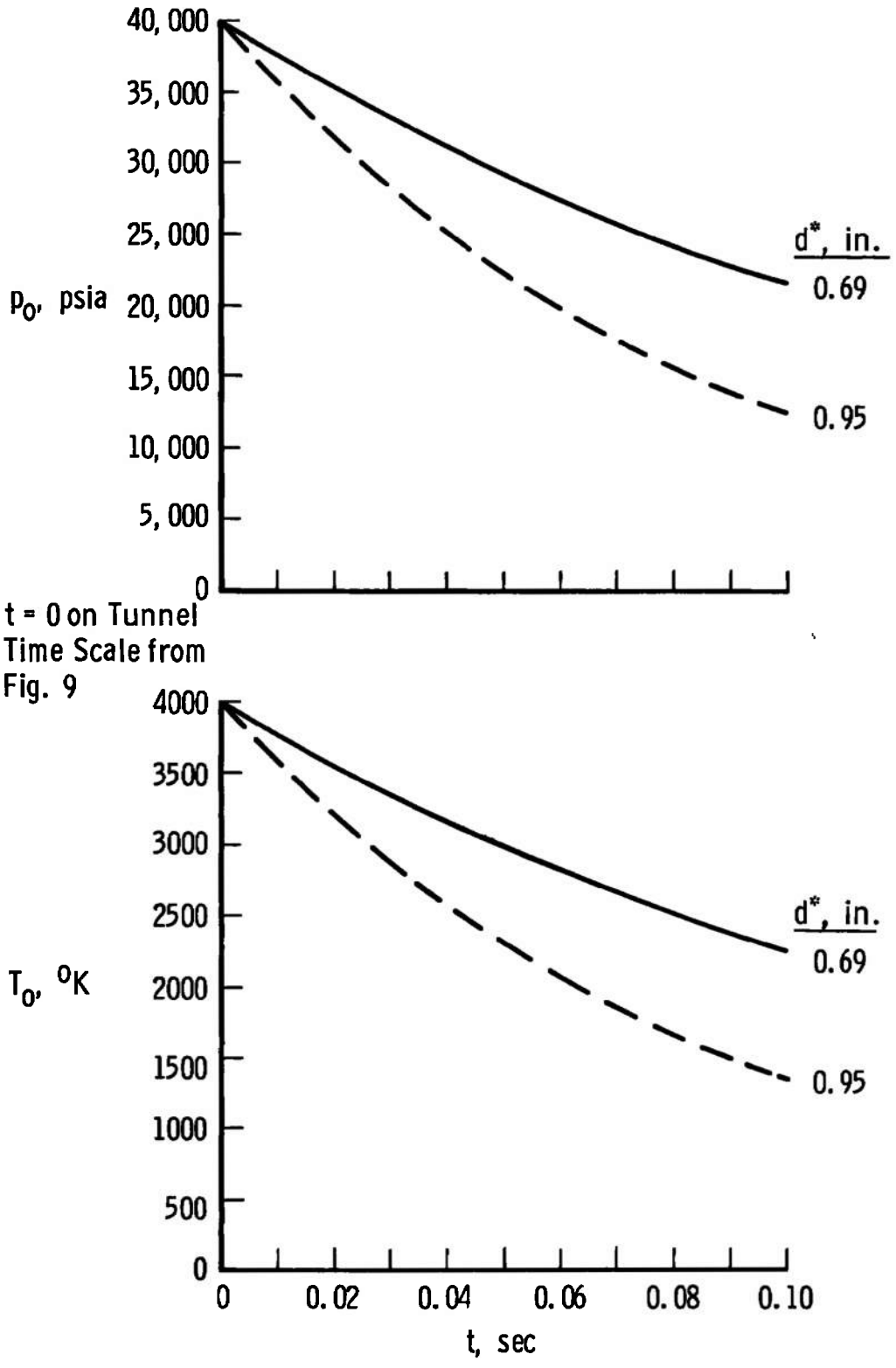

Fig. 19 Estimated Reservoir Decay Rates

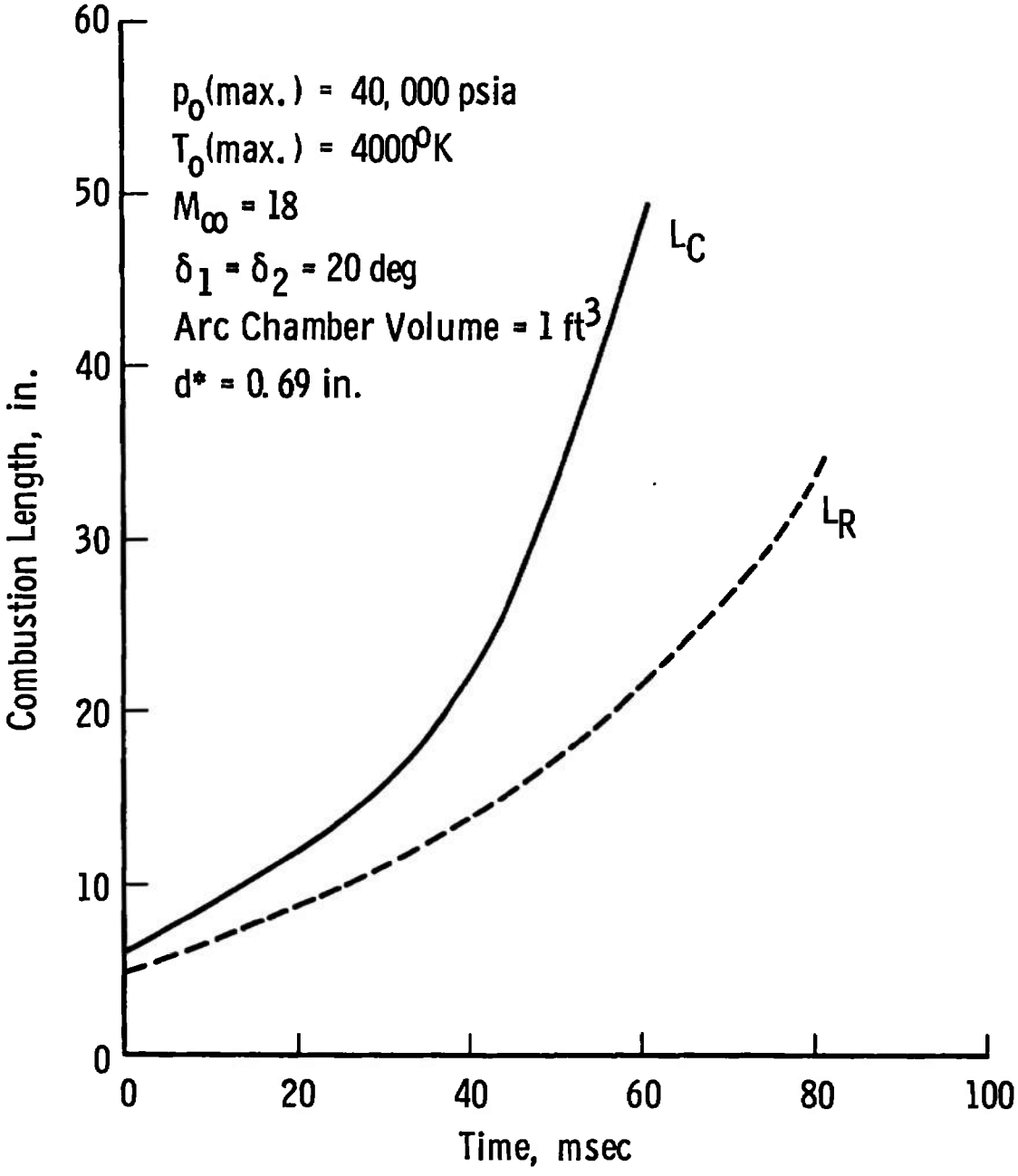

Fig. 20 Variation of Combustion Length with Time (100-in.-diam Test Section) M_∞ = 18

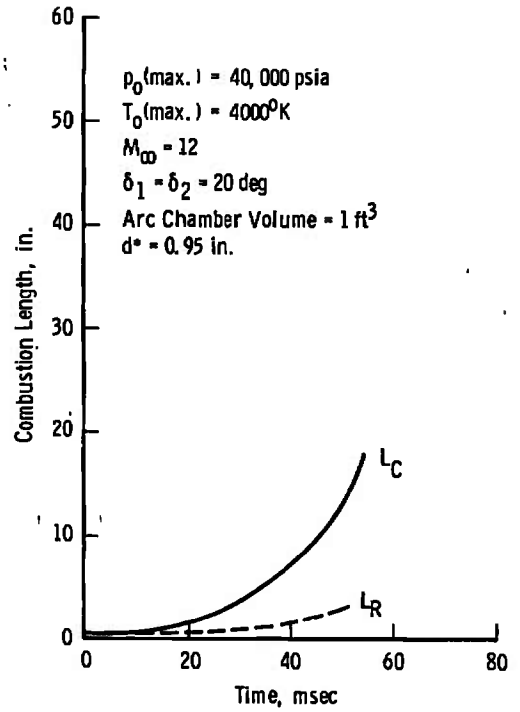

Fig. 21 Variation of Combustion Length with Time (54-in.-diam Test Section) M_∞ = 12

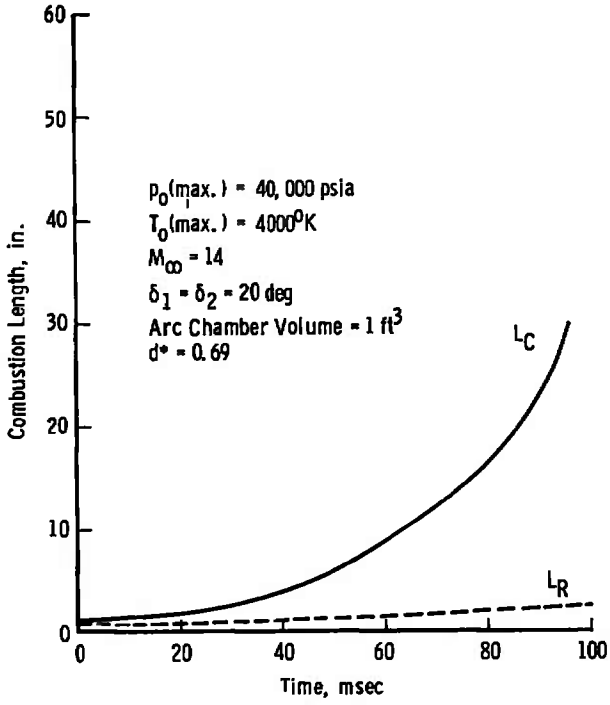

Fig. 22 Variation of Combustion Length with Time (54-in.-diam Test Section) M_∞ = 14

The rates of change of combustion length can be obtained by differentiation of Eqs. (1) and (2), with Eqs. (4) and (5) used to determine the static conditions, and empirical fits of existing data to determine the rates of pressure and temperature decay. These results are summarized in Fig. 23, where again the curves are terminated when the combustor static temperature drops below 1000°K. Assuming that 20 msec are used in the starting process, condition B (M_∞ = 12) offers 25 msec of useful run time, with the latter portion at a marginal static temperature within the combustor. Condition A (M_∞ = 18) offers a longer run time, but from Fig. 20, very large models are required to make full usage of this time. Condition C (M_∞ = 14) offers the possibility of long periods of quasi-steady flow with a reasonable size model; however, the free-stream Mach number is higher than that envisioned for SCRAMjets for the immediate future.

The effect of smaller throat size, which leads to smaller decay rates (see Fig. 19), is seen by comparing Conditions A and B in Fig. 23. Condition C has a greater reservoir pressure and temperature decay rate than Condition A, but is significantly better in terms of the rate of change of combustion length, because of higher pressure recovery at the lower Mach number.

From these results, it appears that the upstream 54-in.-diam test section (Conditions B and C) offers possible conditions with sufficient run time to permit meaningful tests of integrated SCRAMjets; however, further reductions in the reservoir pressure and temperature decay rates are, of course, desirable.

These results also point out that the decay of the arc-chamber pressure and temperature is a more serious limiting factor for combustion testing than for aerodynamic testing, because of the strong dependence of the reaction processes on temperature. Reduction of the reservoir decay rates for the usual hotshot-type tunnel operating from a preheated fixed volume of gas demands, of course, either an increase in arc-chamber volume or a reduction in test section diameter to achieve a given test condition. In view of the adequate capacity of the Tunnel F power supply, a development program to increase arc-chamber volume several fold is now underway.

4.3 IGNITION DELAY

Also shown in Figs. 20, 21, and 22 are the reaction lengths, determined from

$$L_R = U_3 \tau_R$$

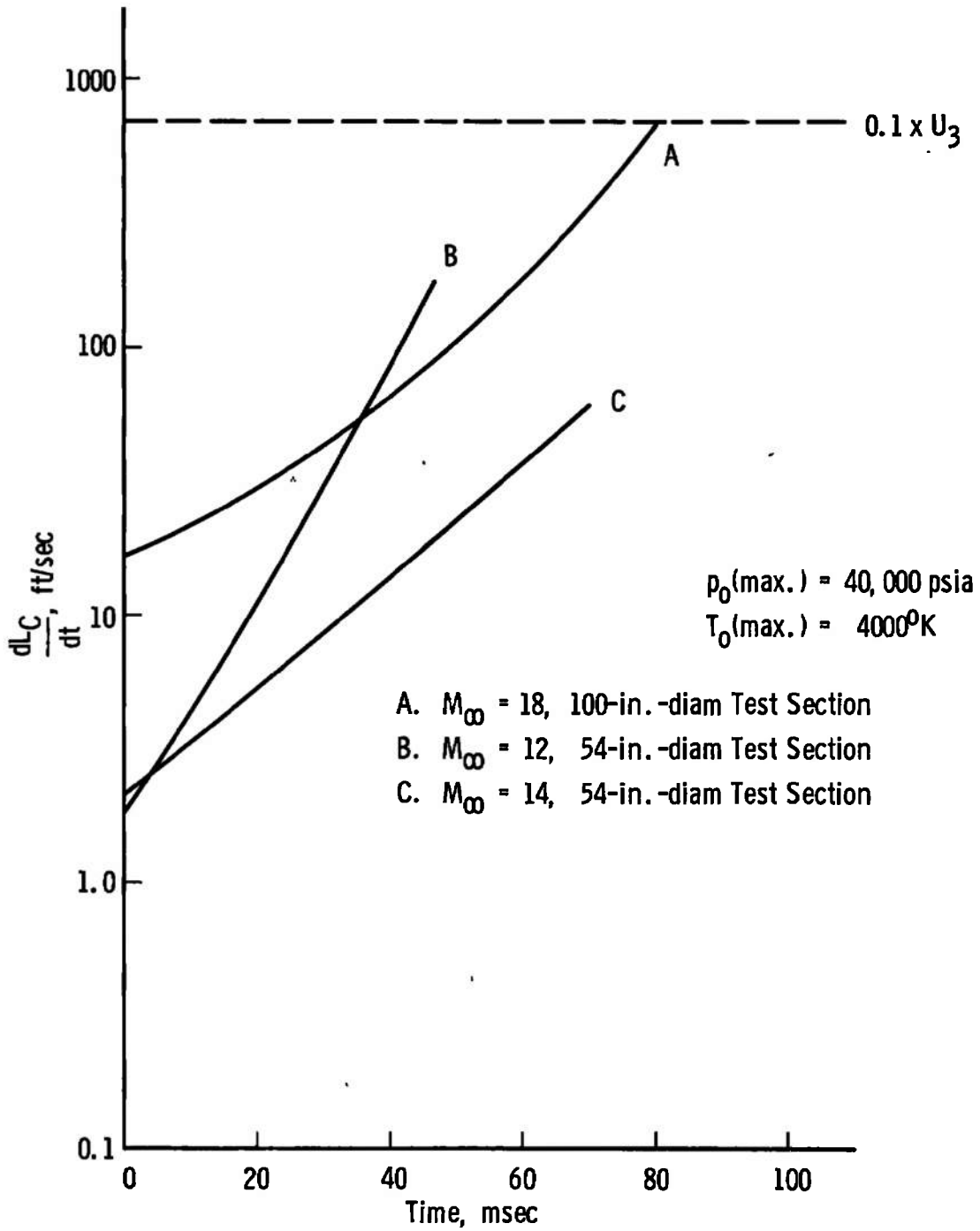

Fig. 23. Variation of Rate of Change of Combustion Length with Time

These curves show that the large increases in combustion length during the test are attributable to the exponential dependence of the ignition delay time on the static temperature, as shown in Fig. 14. Therefore, the validity of the previously presented estimates of combustion length rests strongly on the estimates for the ignition delay (Eq. (1)). The ignition delay time will be influenced by many extraneous factors which have not been considered in the present analysis. It is expected that most of these factors will serve to reduce the ignition delay time; thus, the limitations in test time indicated by the present estimates may not be so severe in practical combustors. Some of the extraneous factors expected to influence the ignition delay time are:

1. Fuel injection ports will have a boundary layer on them which will accelerate local mixing and increase the residence time of fuel and air in the vicinity of the injector.
2. Shock waves are likely to be generated at or near the injector thus increasing the local static pressure and temperature and decreasing the ignition delay.
3. As soon as some fuel ignites, the flame should spread rapidly through unburnt mixtures.

If such is the case, then considerable increases in test time will be possible. It is likely that the mixing delay, which has not been included in the present analysis because of lack of data, is approximately constant, since the mixing rate should be a function primarily of the ratio of the flow velocity to the injected fuel velocity, each of which is relatively constant. In the absence of an ignition delay

$$L_c = L_R - \text{constant}$$

Another factor that deserves mention is the alternate possibility that mixing becomes the dominant process which could lead to large values of the combustion length. The uncertain nature of the ignition and the unknown mixing delay point out the need for detailed experimental analysis.

4.4 EFFECT OF GAS COMPOSITION ON COMBUSTION OF PREMIXED HYDROGEN/AIR

A theoretical study of gaseous contamination has been undertaken in order to determine whether the effects of current contamination levels are significant. Since there are many complex aspects to combustion

testing in Tunnel F, it is again essential to know whether contaminants can produce changes in combustion parameters in addition to those described previously. Two regimes of combustion catalysis can be recognized:

1. Ignition catalysis
2. Reaction catalysis

It has been shown previously that the theoretical ignition delay time and hence ignition length increases exponentially with the reciprocal temperature; thus, if catalysis takes place which significantly reduces the ignition delay, then the combustion length would follow the L_R curves more closely in Figs. 20 through 22. If the reaction length is also altered significantly, then the measured performance of the SCRAMjet model will be altered appreciably by catalysis.

A theoretical model for combustion of premixed hydrogen/air has been used to investigate catalysis. The flow model assumed is similar to the analyses of Refs. 13 through 17: one-dimensional, nonradiating flow. These assumptions are not too restrictive in the present analysis since the approximations introduced should not be affected by pure catalytic effects. For simplicity, constant area flow is also assumed. (It would be difficult to design a constant pressure combustion chamber for quasi-steady conditions considered herein.)

The fluid-dynamic equations solved are those of Ref. 15 since the computer program was already available at AEDC. The chemical kinetics scheme and reaction rates are taken from more recent literature (Refs. 13, 17 through 23).

Chemical Kinetic Scheme for Hydrogen/Air Combustion

$$OH + H_2 \rightarrow H_2O + H \quad (1)$$

$$O_2 + H \rightarrow OH + O \quad (2)$$

$$H_2 + O \rightarrow OH + H \quad (3)$$

$$H + O_2 + M \rightarrow HO_2 + M \xrightarrow{H} 2OH + M \quad (4)$$

$$H + H + M \rightarrow H_2 + M \quad (5)$$

$$H + OH + M \rightarrow H_2O + M \quad (6)$$

Reaction 4 is written as a composite reaction using a reaction rate obtained from Refs. 20 through 23. Thermodynamic data are tabulated in Ref. 24, and polynomial equations have been fitted to the data.

This kinetic scheme is suitable for investigating the effects of oxygen depletion and the presence of water. Oxygen concentrations of 20.9 percent (dry air), 20 percent, 19 percent, 18 percent, and 16 percent (by volume) are considered to be representative of the air analyses obtained in Tunnel F. The hydrogen concentration was maintained constant for all calculations and corresponds to a stoichiometric mixture for the 20.9-percent oxygen case.

In Fig. 24, the effect of oxygen concentration on the hydrogen atom concentration along the duct is shown. The ignition delay, which is determined by the position of maximum hydrogen atom concentration (Ref. 25), is seen to be affected only slightly by oxygen depletion. The oxygen depletion cases do indicate a change in heat release rate and pressure rise (Figs. 25 and 26) along the combustor. These differences would probably be difficult to isolate from factors mentioned previously in all but the lower oxygen concentrations.

Calculations using the water concentrations found in air samples from Tunnel F tests (Table I) revealed no significant changes in the ignition delay or heat release rate.

SECTION V
CONCLUSIONS

Experiments carried out in Tunnel F using air as a test gas indicate that:

1. There is small oxygen depletion for operation at total temperatures up to 3000°K.
2. Particle contamination and flow uniformity with air as the test gas are not significantly different from those obtained using nitrogen as the test gas.
3. The effects of quasi-steady total conditions show a marked dependence of ignition delay on total temperature decay.
4. Test times in excess of 20 msec may be obtained at the 54-in.-diam test section with the present Tunnel F arc-chamber. A larger arc-chamber will offer a much broader combustion test capability.
5. Theoretical calculations indicate that small oxygen depletion (< 3 percent) and water vapor concentrations (< 1 percent) do not appreciably influence the combustion process.

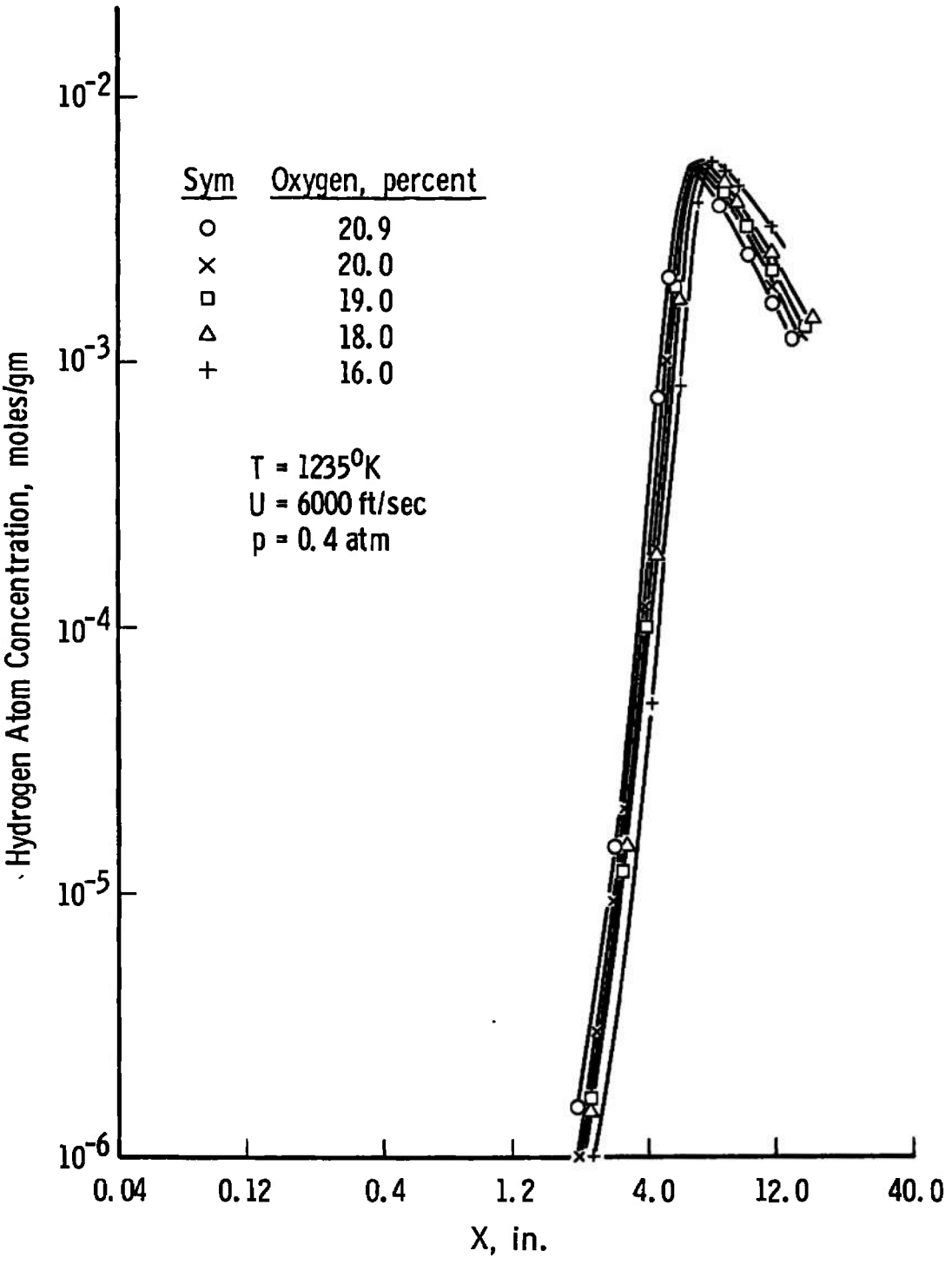

Fig. 24 Effect of Oxygen Depletion on the Concentration of Hydrogen along a Duct

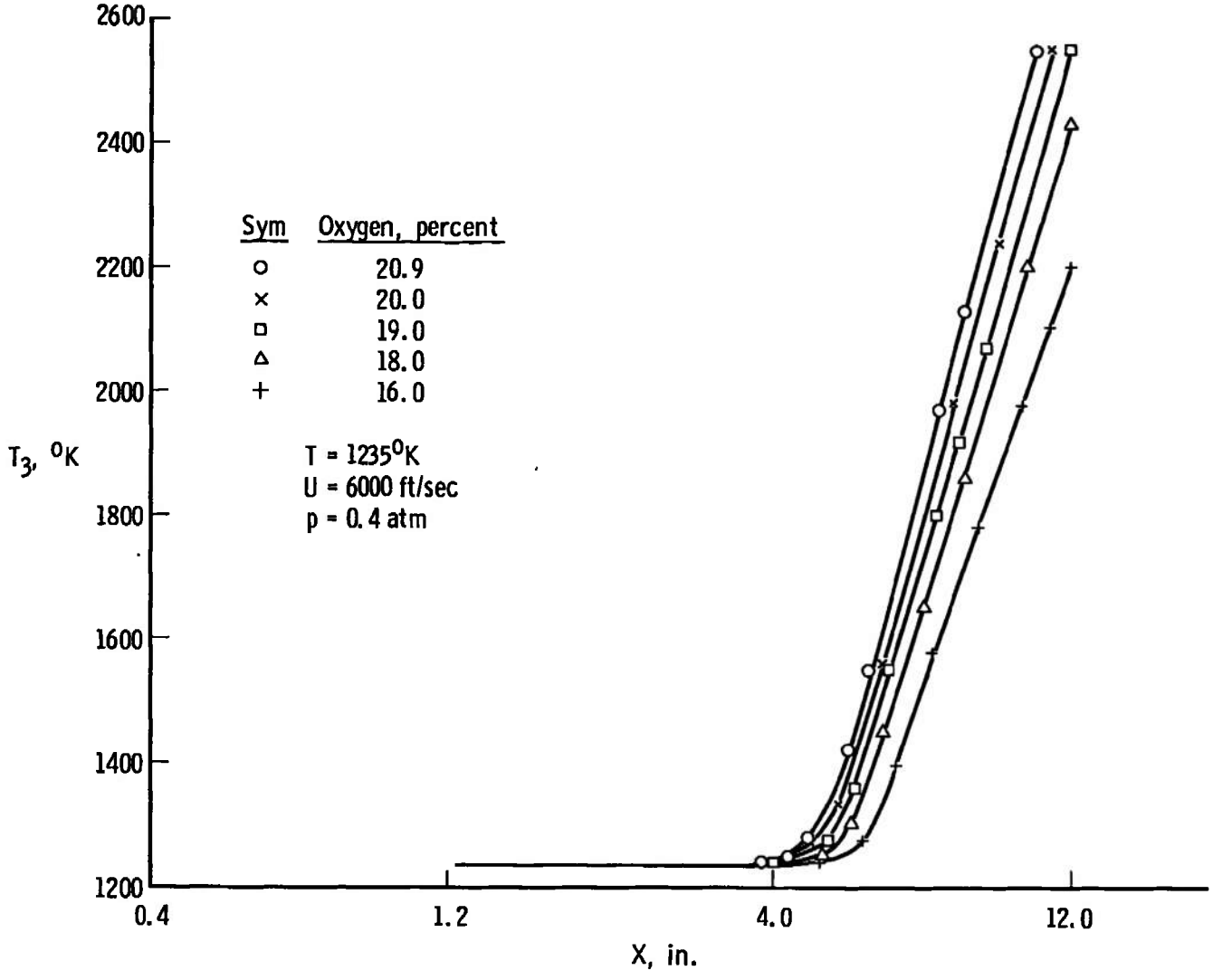

Fig. 25 Effect of Oxygen Depletion on the Temperature Distribution along a Duct

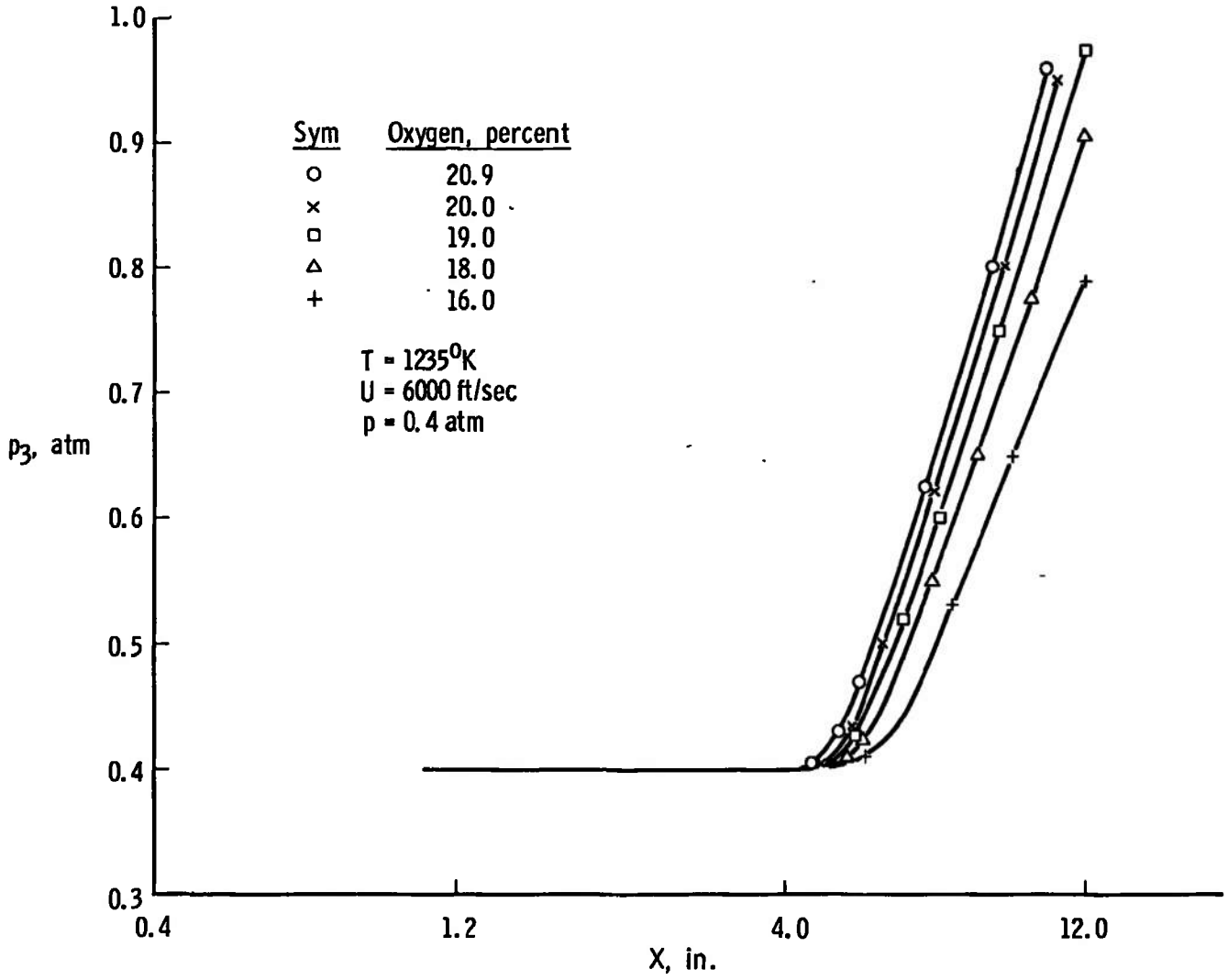

Fig. 26 Effect of Oxygen Depletion on the Pressure Distribution along a Duct

REFERENCES

1. Ball, H. W. "Calibration of the 100-inch Hypervelocity Tunnel F." AEDC-TDR-63-46 (AD298279), March 1963.
2. Griffith, B. J. and Weddington, E. D. "Calibration and Status of the AEDC-VKF 100-in. Hotshot Tunnel (F)." AEDC-TR-66-191 (AD800778), October 1966.
3. Whitfield, J. D. and Griffith, B. J. "Hypersonic Viscous Drag Effects on Blunt Slender Cones." AIAA Journal, Vol. 2, No. 10, October 1964, pp. 1714-1722.
4. Whitfield, J. D. and Wolny, W. "Hypersonic Static Stability of Blunt Slender Cones." AEDC-TDR-62-166 (AD282897), August 1962. (Also AIAA Journal, Vol. 1, No. 1, February 1963, p. 486.)
5. Whitfield, J. D. and Griffith, B. J. "Comparisons of Free Flight and Wind-Tunnel Data on Slender Cones." AIAA Journal, Vol. 3, No. 3, February 1965, pp. 379-380.
6. Griffith, B. J. and Siler, L. G. "Comparisons of Free-Flight and Wind Tunnel Data on Slender Cones." AEDC-TDR-64-272 (AD453414), December 1964.
7. Griffith, B. J. and Lewis, Clark H. "Laminar Heat Transfer to Spherically Blunted Cones at Hypersonic Conditions." AIAA Journal, Vol. 2, No. 3, March 1964, pp. 438-444.
8. Eaves, R. H., Jr., and Lewis, Clark H. "Combined Effects of Viscous Interaction and Source Flow on Pressure and Heat Transfer Distributions over Hemisphere Cylinders at M_∞ - 18." AEDC-TR-65-158 (AD467447), July 1965.
9. Lukasiewicz, J., Harris, W. G., et al. "Development of Capacitance and Inductance Driven Hotshot Tunnels." AEDC-TN-60-222 (AD249421), January 1961.
10. Ledford, R. L., Smotherman, W. E., and Kidd, C. T. "Recent Developments in Heat Transfer Rate, Pressure and Force Measurements for Hotshot Tunnels." Paper presented at the Second International Congress on Instrumentation in Aerospace Simulation Facilities, Stanford University, August 29-31, 1966.
11. Pergament, H. S. "A Theroretical Analysis of Non-Equilibrium Hydrogen-Air Reactions in Flow Systems." AIAA-ASME Hypersonic Ramjet Conference, Naval Ordnance Lab., White Oak, Maryland, April 1963.

12. Equations, Tables, and Charts for Compressible Flow. NACA 1135, 1953.

13. Osgerby, I. T. "Supersonic Combustion and Turbulent Jet Mixing. Ph.D Thesis, Department of Fuel Tech. and Chem. Eng., Sheffield University, England, October 1965.

14. Momtchiloff, I. N. et al. "Calculation of Ignition Delays for Hypersonic Ramjets." Ninth Symposium (Int.) on Combustion, Academic Press, 1963.

15. Westenberg, A. A. and Favin, S. "Complex Chemical Kinetics in Supersonic Nozzle Flow." Ninth Symposium (Int.) on Combustion, Academic Press, 1962.

16. Fowler, R. G. "Theoretical Study of Hydrogen-Air Reaction." Proceedings Heat Transfer and Fluid Mechanics Inst., Stanford University Press, 1962.

17. Ferri, A. et al. "Theoretical and Experimental Investigation of Supersonic Combustion." Third Int., Congress on Aeronautical Science, Stockholm, August 1962.

18. Elliss, G. E. and Bahn, G. S. "Engineering Selection of Reaction Rate Constants for Gaseous Chemical Species at High Temperatures." 1962 Fall Meeting, Western States Section, The Combustion Institute, November 1962.

19. Schott, G. L. and Bird, P. F. "Kinetic Studies of Hydroxyl Radicals in Shock Waves. IV: Recombination Rates in Rich Hydrogen/Oxygen Mixtures." Chemical Physics, Vol. 41, No. 9, November 1964.

20. Getzinger, R. W. and Schott, G. L. "Kinetic Studies of Hydroxyl Radicals in Shock Waves. V: Recombination via the $H + O_2 + M \rightarrow HO_2 + M$ Reaction in Lean Hydrogen/Oxygen Mixtures." J. Chem. Phys., Vol. 43, No. 9, November 1965.

21. Getzinger, R. W. "A Shock Wave Study of Recombination in Near Stoichiometric Hydrogen/Oxygen Mixtures." Eleventh Symposium (Int.) on Combustion, 1966.

22. Basevitch, V. Ya and Kogarko, S. M. "Flame Propagation under Conditions of an Ignition Peninsular of Hydrogen/Oxygen Mixtures." Kinetiku i Kataliz. (Russian) Vol. 6, No. 1, 1965. Also FTD-TT-65-919/1+2+4.

23. Strehlow, R. G., University of Illinois, Private Communication.

24. J. A. N. A. F. Thermochemical Tables, Thermal Research Laboratory, Dow Chemical Company, Midland, Michigan, 1965.

25. Nicholls, J. A. "Stabilization of Gaseous Detonation Waves with Emphasis on the Ignition Delay Zone." Ph. D Thesis, University of Michigan, January 1960.

Security Classification

DOCUMENT CONTROL DATA - R & D

(Security classification of title, body of abstract and indexing annotation must be entered when the overall report is classified)

1. ORIGINATING ACTIVITY *(Corporate author)*
Arnold Engineering Development Center
ARO, Inc., Operating Contractor
Arnold Air Force Station, Tennessee

2a. REPORT SECURITY CLASSIFICATION
UNCLASSIFIED

2b. GROUP
N/A

3. REPORT TITLE
OPERATION OF AEDC-VKF 100-IN. HOTSHOT TUNNEL F WITH AIR AS A TEST GAS AND APPLICATION TO SCRAMJET TESTING

4. DESCRIPTIVE NOTES *(Type of report and inclusive dates)*
January 1966 through May 1967

5. AUTHOR(S) *(First name, middle initial, last name)*
I. T. Osgerby and H. K. Smithson, ARO, Inc.

6. REPORT DATE	7a. TOTAL NO. OF PAGES	7b. NO. OF REFS
December 1967	44	25

8a. CONTRACT OR GRANT NO.
AF 40(600)-1200

b. PROJECT NO. 3012

c. Program Element 6240521F

d. Task 301207

9a. ORIGINATOR'S REPORT NUMBER(S)
AEDC-TR-67-242

9b. OTHER REPORT NO(S) *(Any other numbers that may be assigned this report)*
N/A

10. DISTRIBUTION STATEMENT
This document has been approved for public release and sale; its distribution is unlimited.

11. SUPPLEMENTARY NOTES
Available in DDC

12. SPONSORING MILITARY ACTIVITY
Arnold Engineering Development Center, Air Force Systems Command
Arnold Air Force Station, Tennessee

13. ABSTRACT

An experimental and theoretical research program has been undertaken to develop the arc-heated hypervelocity Tunnel F of the von Kármán Gas Dynamics Facility (AEDC) for operation as a combustion test facility with air as a test gas. Preliminary results of this test program are reported concerning gaseous and particle contamination and the limitations on combustion testing attributable to reservoir decay.

DD FORM 1 NOV 65 1473

Security Classification

14 KEY WORDS	LINK A		LINK B		LINK C	
	ROLE	WT	ROLE	WT	ROLE	WT
SCRAMJET Testing wind tunnels test gas - air						